1
Introduction

1.1 LAYERED 2D MATERIALS

The 2D materials provide an edge over other low dimensional materials (0D and 1D) due to their layer by layer interaction, which gives birth to new exciting physics. The 2D materials possess a large number of electronic, optical, chemical, and thermal properties which have never been seen in their 3D counterpart(Wang et al., 2014). In layered 2D materials, different atoms are held by a strong covalent bond in a single atomic layer, while different layers are bonded together by a weak van der Waals force. Such a weak van der Waals force between adjacent layers allows cleavage of a few-layer to monolayer of a material through mechanical exfoliation or liquid phase exfoliation methods(Li et al., 2013; Nicolosi et al., 2013). The tremendous increase in the number of the publication since 2004 is the manifestation of their popularity. In 2004, 1245 articles were published related to 2D materials, which reaches 8330 in the year 2019, as shown in Figure 1.1. Due to increasing research interest, all classes of 2D materials varying from insulator to superconductor have been discovered, as depicted in Figure 1.2(Kang et al., 2014).

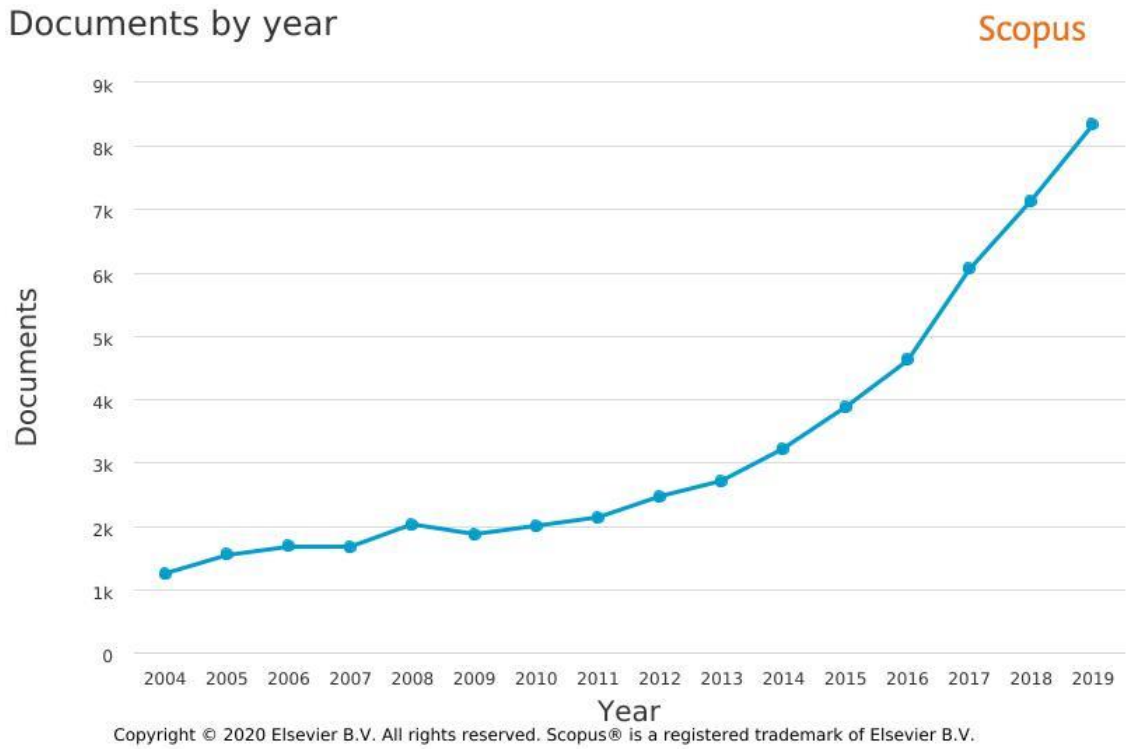

Figure 1.1: The rapidly increasing number of publications on 2D materials with each passing year. (Source: Scopus)

The distinct properties of 2D materials simulated the researcher's interest in exploring various synthesis methods to grow large-scale atomically thin layers of these materials. The most commonly used synthesis methods are- mechanical exfoliation, liquid exfoliation, chemical vapor deposition (CVD), pulsed laser deposition (PLD), and hydrothermal processes.

Although with the advancement of time, some modification has been introduced into these existing techniques to improve the quality and area of synthesized 2D materials(Huang et al., 2015; Wong et al., 2016). Different preparation techniques might result in different nanostructures. These different structures might change the surface properties and hence the physical and chemical properties of a particular material. Therefore, for a deeper understanding of the functionalities of grown 2D structures, advanced microscopic and spectroscopic characterization techniques are required. Field emission scanning electron microscopy (FE-SEM), atomic force microscopy (AFM), optical microscopy, X-ray photoelectron spectroscopy (XPS), Ultraviolet Photoelectron Spectroscopy (UPS), and Raman characterization are few commonly used techniques to study physical, chemical, and electronic properties of the 2D materials.

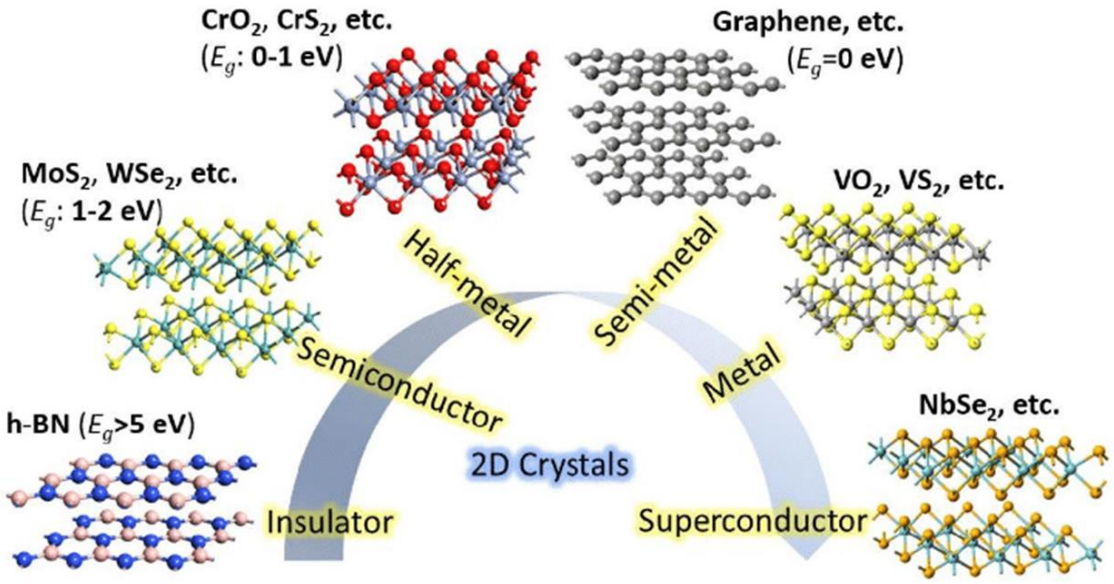

Figure 1.2: Different classes of 2D materials varying from insulating to superconducting behavior. (Source: Kang et al., 2015)

The 2D materials have numerous unique features which never exist in their 3D counterpart. Quantum confinement in single or few-layer ultrathin materials is one such feature leading to a new exciting physics in next-generation devices(Favron et al., 2015). The other feature includes atomic thickness and strong covalent bond within a plane resulting in transparency, flexibility, and mechanical strength of electronic devices. Moreover, apart from the above mentioned unique features, very large surface to volume ratio and solution processability also makes them special in condenced matter physics(Lee et al., 2013; Lin et al., 2018). The large surface area is particularly useful in surface applications, for example, gas sensing applications. While the solution processability helps in achieving the free-standing thin films for solar applications. Due to their distinct features, these 2D materials have found their applications in most of the fascinating research areas such as material science, engineering, physics, chemistry, computer science, medicine, and energy, etc. as depicted in Figure 1.3. It is clear from Figure 1.3 that materials science and engineering fields cover the major part of the ongoing research in the field of low dimensional materials.

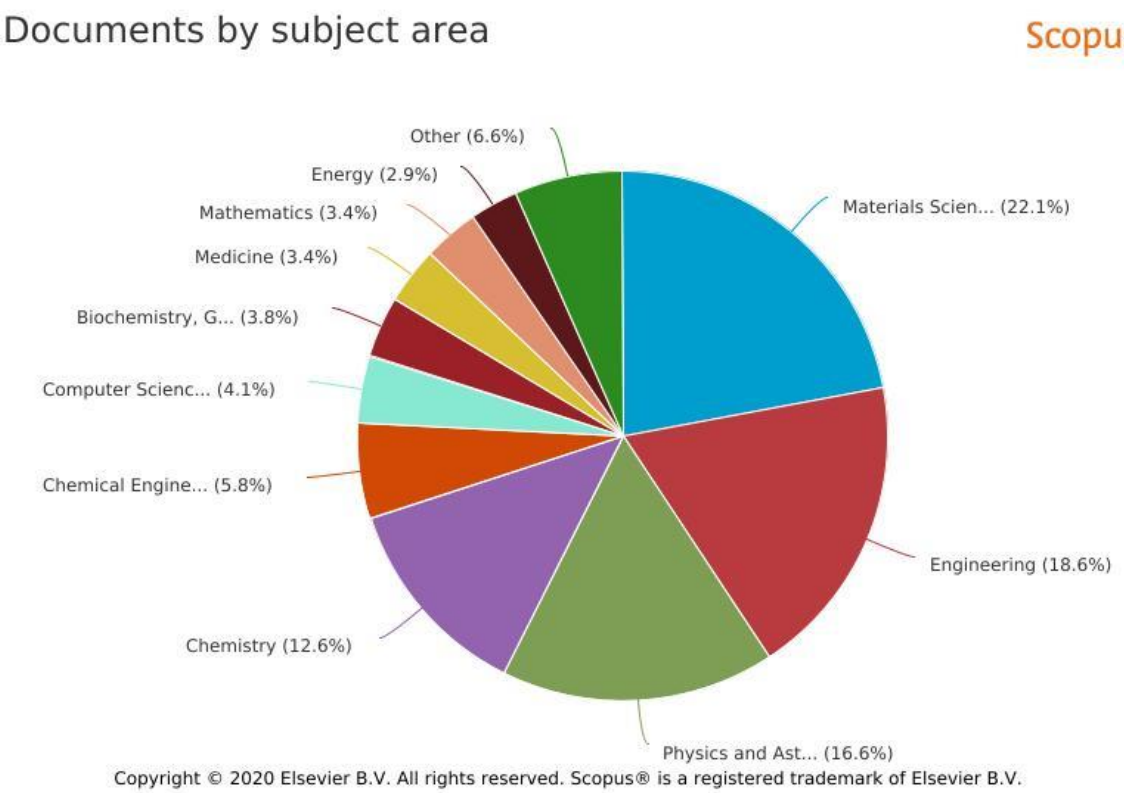

Figure 1.3: Research done on 2D materials in different disciplines. (Source: Scopus)

In optoelectronic applications, the light interacts strongly with atomically thin 2D materials making them suitable for light detection and modulation applications. Different classes of 2D materials cover a different range of electromagnetic spectrum depending on their specific properties, as shown in Figure 1.4(Xia et al., 2014). Graphene is used for a broad spectral range because of its semi-metallic nature. TMDs such as MoS2 shows the promising light-emitting behavior from visible to near-infrared range. Hexagonal boron nitride used as a perfect 2D dielectric due to the availability of large bandgap. Black phosphorus also shows encouraging light sensing properties from visible to infrared region. By combining materials with different spectral ranges, researchers have realized different nanophotonic devices for different applications.

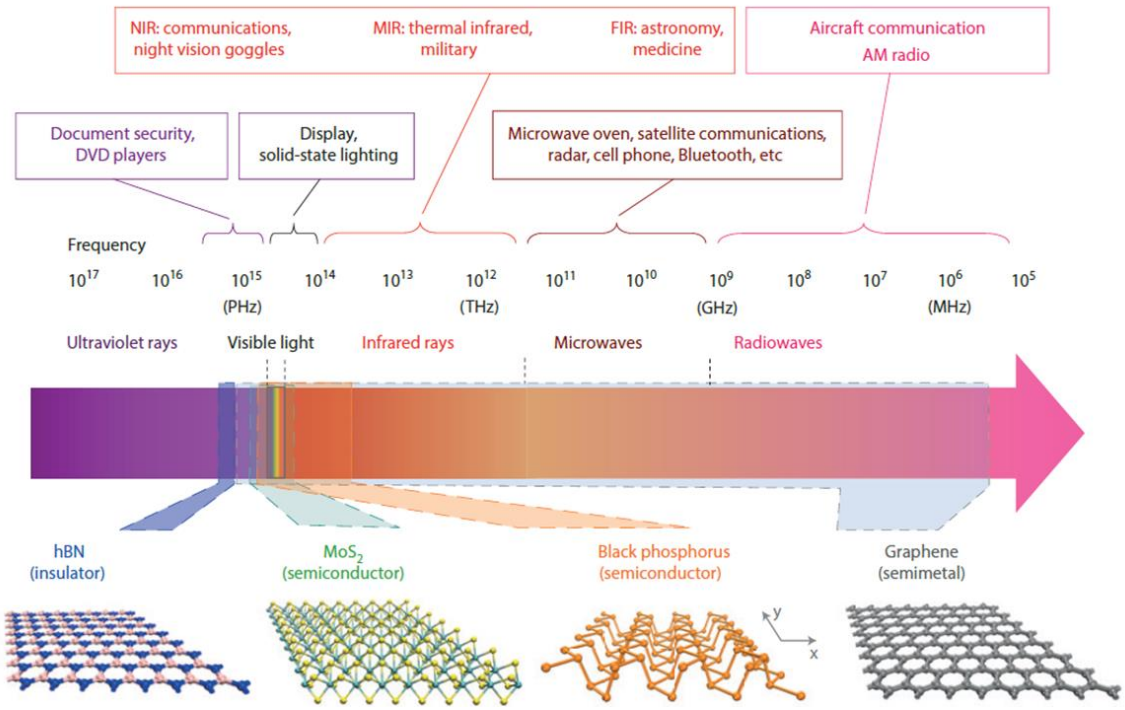

Figure 1.4: The different spectral range covered by various 2D materials. (Source: Xia et al., 2014)

It is difficult to say how much time these 2D materials will take to move from research labs to the commercial platform. Borophene, germanene, silicene, stanene, plumbene, and phosphorene are some of the newly discovered 2D materials. In the last few years, these 2D materials have toughed every sphere in material science, for instance, insulator (hexagonal BN), semiconductors (MoS_2, WS_2, etc.), semi-metal (graphene), metals (VO_2, VS_2, etc.), and superconductor (NbS_2, $NbSe_2$, etc.). Depending on a particular application, a specific 2D materials can be chosen which fulfill the desired set of conditions. These newly generated 2D materials are so fascinating that even in some particular applications, they have outperformed graphene also. Figure 1.5 shows the major milestone achieved in the history of 2D materials starting from the birth of graphene in 2004. However, most of the newly discovered 2D materials are in their nascent stage, and multidisciplinary efforts are required to explore the full potential of these materials.

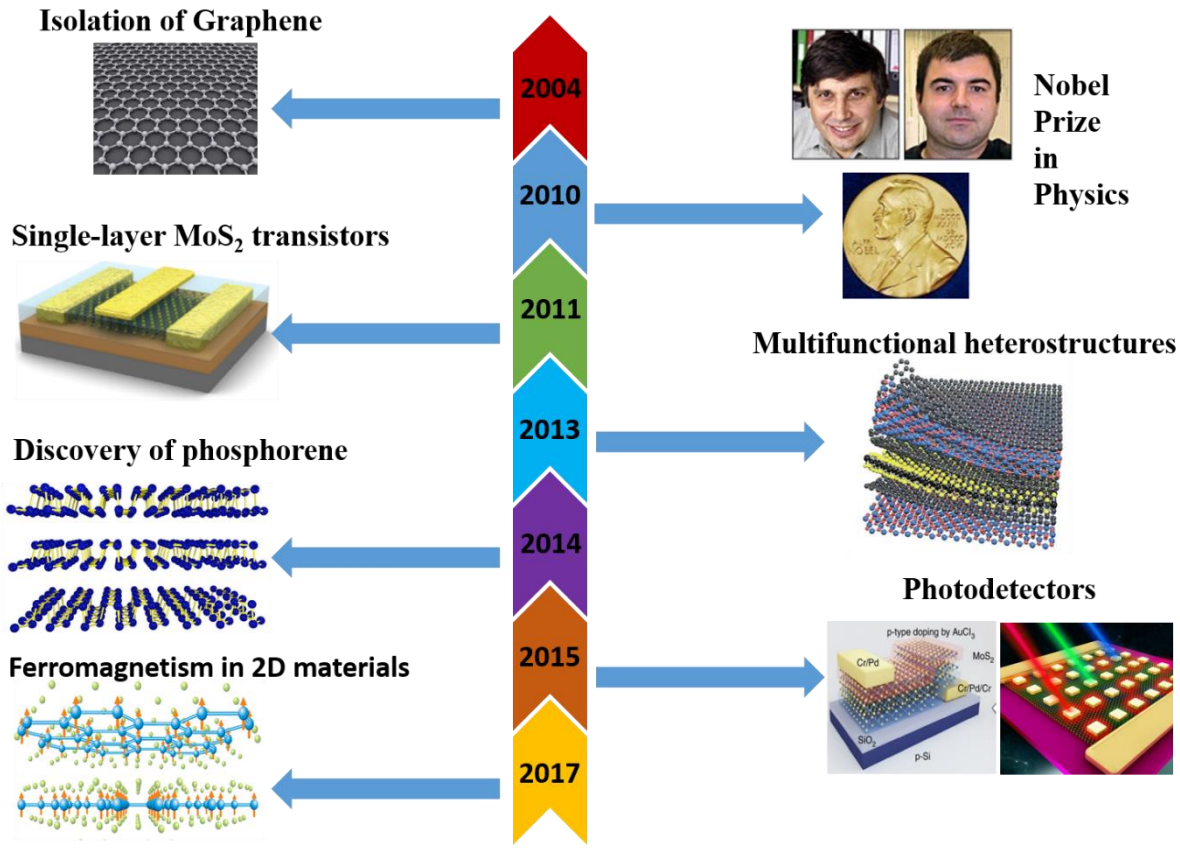

Figure 1.5: Milestones achieved in the field of 2D materials starting from graphene.

In this chapter, we will extensively explain the 2D materials and their recent advances in the field of optical and gas sensors. Various types of 2D materials, including insulating, semiconducting, and metallic, will be studied in detail, focusing on their specific advantages. Starting from graphene, we will touch the other newly developed 2D materials such as phosphorene, borophene, hexagonal boron nitride, and TMDs. Further, we precisely explain the heterostructures formed by combining different dimensional materials. We elaborate on the suitability of these heterostructures for high-performance photo and gas sensing applications. Nowadays, these heterostructures play a vital role in addressing the problems of our daily life.

1.2 GRAPHENE

In 2004, prof. Andre Konstantin Geim and Konstantin Sergeevich Novoselov obtained the single layer of graphite called graphene. The single-atom thin layer was obtained through

the mechanical exfoliation technique. It consists of covalently bonded carbon atoms in a hexagonal 2D structure and serves as the basis of other-dimensional carbon materials, as shown in Figure 1.6(Novoselov and Geim, 2007). The two carbon atoms are separated by a distance of around 1.42 A˚ in single-layer graphene. And the different layers are stick together by a weak van der Waals force heaving a distance of around 3.35 A˚ between the two layers(Alam et al., 2011). Graphene exhibits unique physical, electronic, mechanical, and chemical properties due to the quantum confinement effect. Graphene is highly conducting material because of its exceptionally high mobility of charge carriers and zero value of bandgap(Shishir and Ferry, 2009). Several researchers tried their level best to introduce a bandgap into the graphene by various strategies. But they have to compromise on intrinsic properties of graphene, particularly the charge carrier mobility. Giovannetti et al. have opened a bandgap of 53 meV into graphene by growing graphene on top of hexagonal boron nitride(Giovannetti et al., 2007). However, bandgap opening increases the complexity, edge roughness, and significantly reduces the mobility of graphene. Xia et al. have also introduced a bandgap of around 130 meV into bilayer graphene by applying a perpendicular electric field(Xia et al., 2010). A current on/off ratio of 100 was achieved at room temperature, while it was 2000 at 20 K temperature. This value of on/off current can further be improved by improving the strength of the gate dielectric and the quality of bilayer graphene. But again, this bandgap opening is at the cost of a very high voltage.

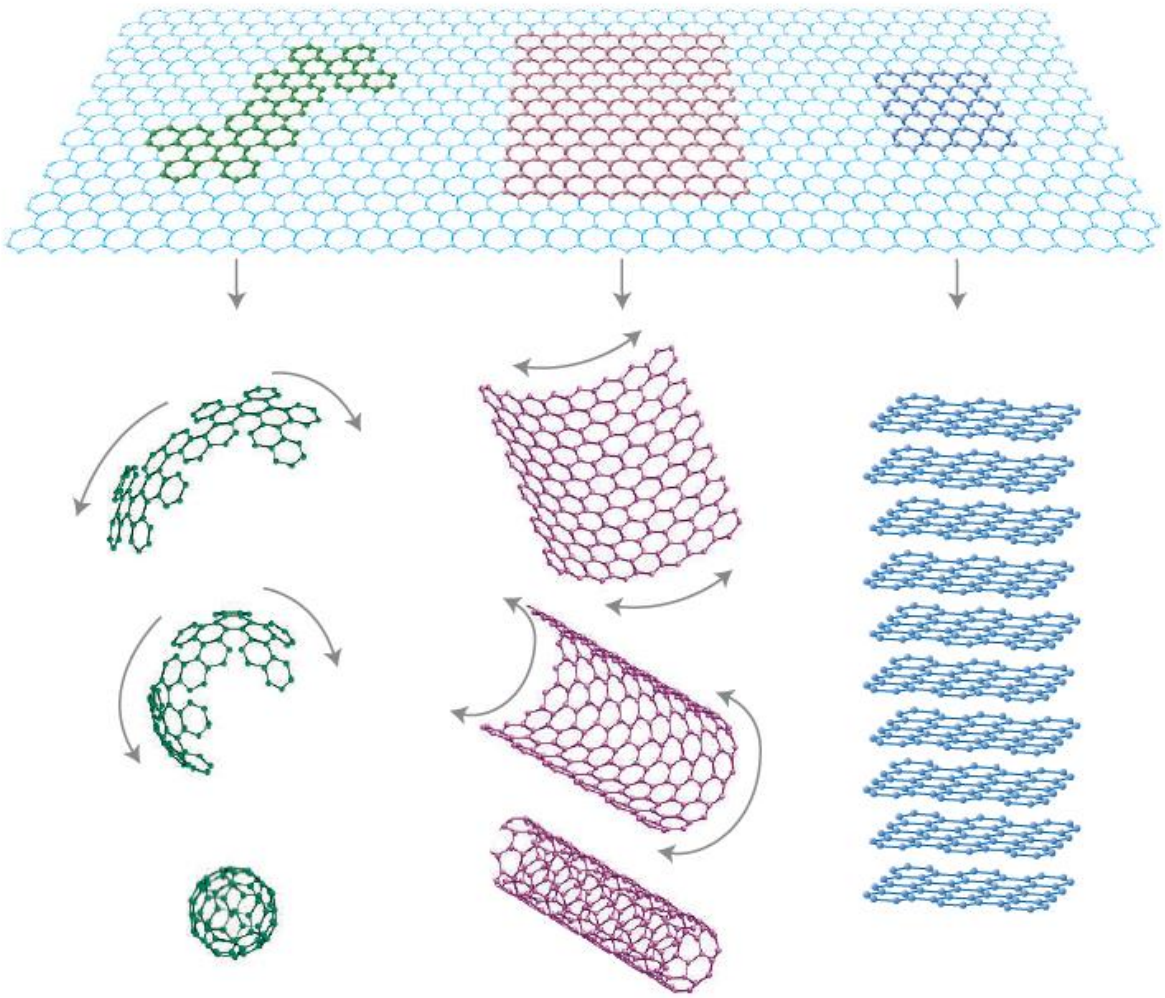

Figure 1.6: The first discovered 2D material, graphene, in 0D, 1D, and 3D forms. (Source: Geim and Navoselov, 2007)

Due to its unique structural properties and band structure, electrons behave like massless Dirac Fermions in graphene(Novoselov et al., 2005). This peculiar feature of graphene leads to the study of several physical phenomena, for example, Klein tunneling and quantum

hall effects. Klein tunneling is shown in Figure 1.7, depicting tunneling of an electron from the conduction band to the valance band. The absence of backscattering makes the graphene highly conductive(Zhang et al., 2014). However, these features disappear beyond three layers of graphene thickness. In graphene, electrons can easily travel a distance of the order of micrometers. The large distance traveling without any scattering confirms excellent carrier mobility and very high electrical conductivity. The room temperature mobility of graphene is measured to be ~ 10000 $cm^2/V.s$. Lee et al. have measured the breaking strength of pristine graphene to be 42 N/m, making it the strongest material ever existed(Lee et al., 2008). In addition, it can be bent up to 20 % without any breakage confirming its excellent flexibility.

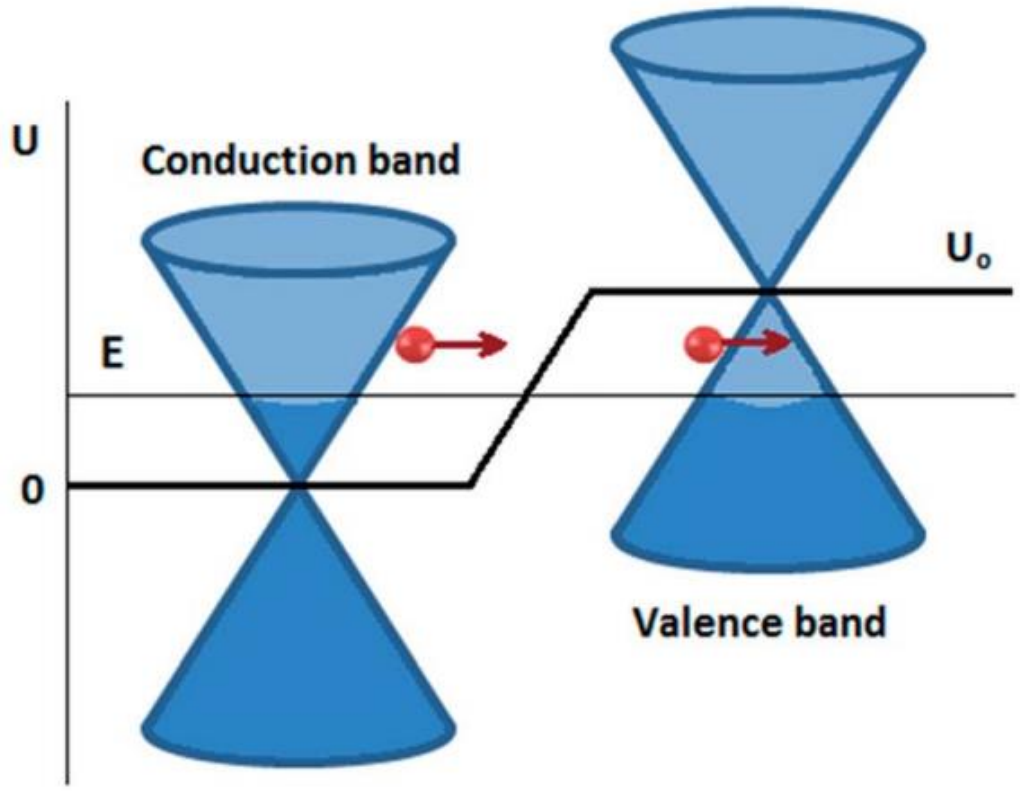

Figure 1.7: Klein tunneling effect in graphene. (Source: Zhang et al., 2014)

Graphene has shown its very promising gas sensing ability because of its atomic thin structure resulting in a very high surface to volume ratio. In 2007, Schedin et al. have detected single gas molecules attached to the graphene's surface(Schedin et al., 2007). To preserve the intrinsic quality of graphene, it was obtained through the mechanical exfoliation technique. The adsorbed single gas molecules change the carrier concentration of the graphene's surface, resulting in a change in resistance, as shown in Figure 1.8(b). The exceptionally low noise ability present in graphene devices drives it to achieve such a high value of sensitivity. The sensor also shows a very fast response upon adsorption and desorption of a single NO_2 molecule (Figure 1.8(b)). This excellent sensing behavior of graphene attracted huge research not only on graphene but also on other 2D materials in the field of gas sensing.

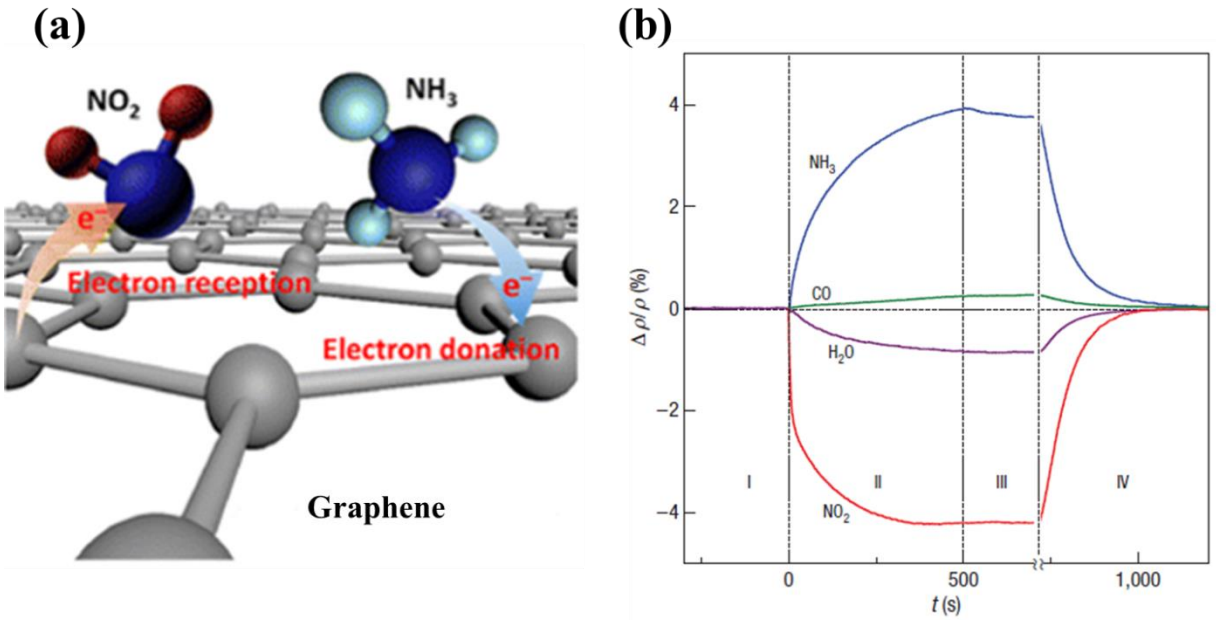

Figure 1.8: (a) Schematic illustration and (b) resistivity changes upon exposure to different gas molecules on the graphene surface. (Source: Schedin et al., 2007)

In communication and photo-sensing applications, it is always desirable to use materials that detect light over a wide wavelength range. The ability of graphene to cover a broad spectral range makes it suitable for promising photodetection applications. Graphene covers a wide range of absorption varying from ultraviolet to far-infrared range(Mak et al., 2012). However, graphene photo-sensing performance is limited due to its poor optical absorption. Therefore, several researchers tried to improve the optical performance of graphene using several techniques.

Liu et al. have overcome this shortcoming of graphene using a double-layer graphene structure, as shown in Figure 1.9(a)(Liu et al., 2014). The top layer works as a gate, while the bottom layer functions as a channel. Both top and bottom layers of graphene are separated by a very thin layer of Ta_2O_5. Under optical irradiation, photoinduced charge carriers generated in the top layer. These photoinduced carriers tunnel across the barrier and reach the bottom graphene layer. The movement of photoinduced charge carriers between the top and bottom layers of graphene is shown by the energy band diagram, as displayed in Figure 1.9(b). Therefore, a positive charge appears on top of gate layer resulting in a strong photogating effect on the bottom channel layer. The gate modulated photocurrent under 532 nm light irradiation is shown in Figure 1.9(c). The photocurrent increases with an increase in illumination intensity. Gate tunability of the photocurrent makes the device convenient for on/off control. Photorespinsivity of the device is displayed in Figure 1.9(d). A photoresponsivity of ~10^3 A/W was achieved, which is never possible to be obtained using a single layer pristine graphene. These results confirm the suitability of graphene-based photodetectors for promising optoelectronic applications.

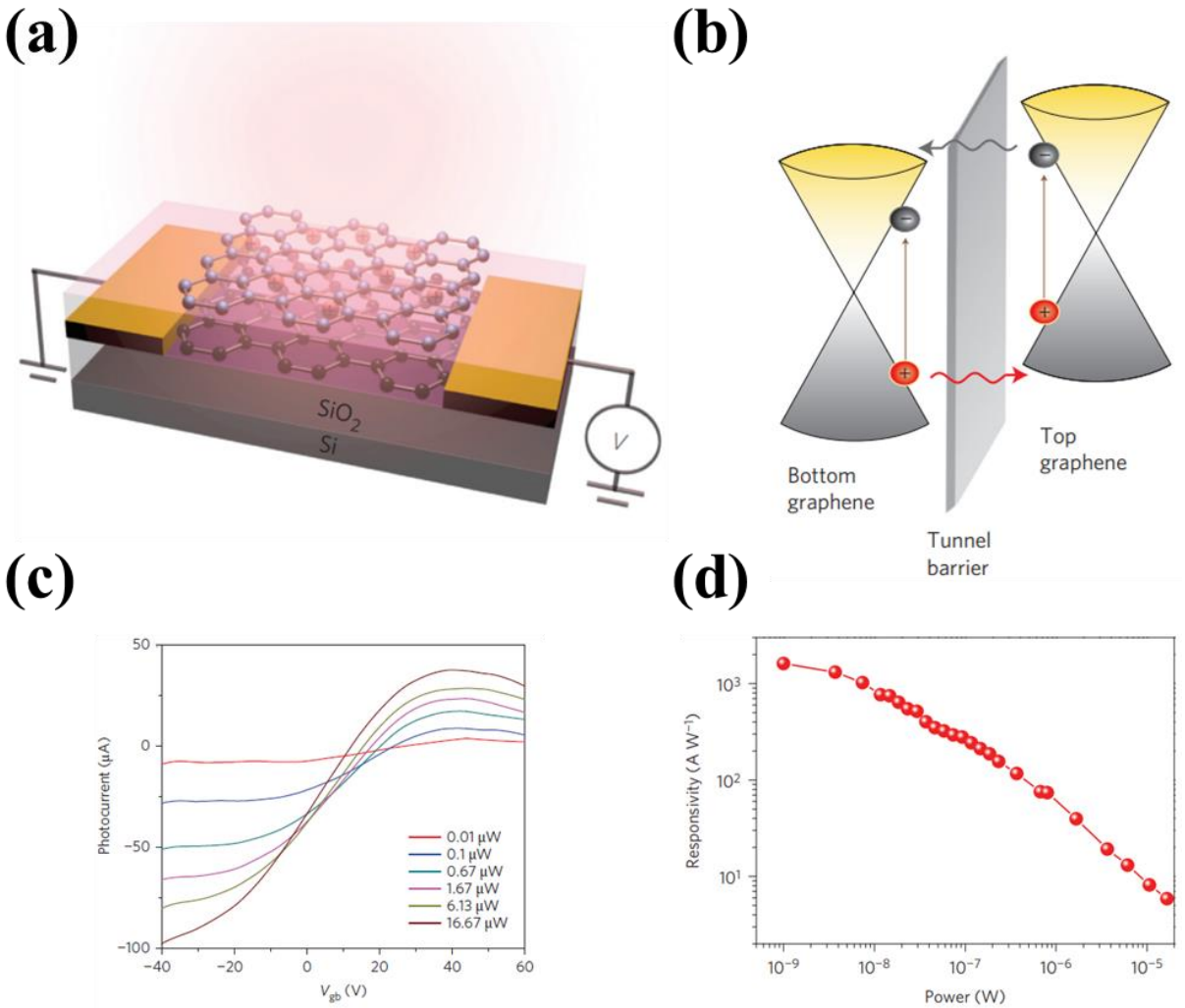

Figure 1.9: (a) Schematic illustration of double-layer graphene photodetector. (b) Band alignment and photoinduced carrier movement between the bottom and top layer of graphene. (c) Gate tunable photocurrent with varying illuminating power. (d) Photoresponsivity at different values of laser power. (Source: Liu et al., 2014)

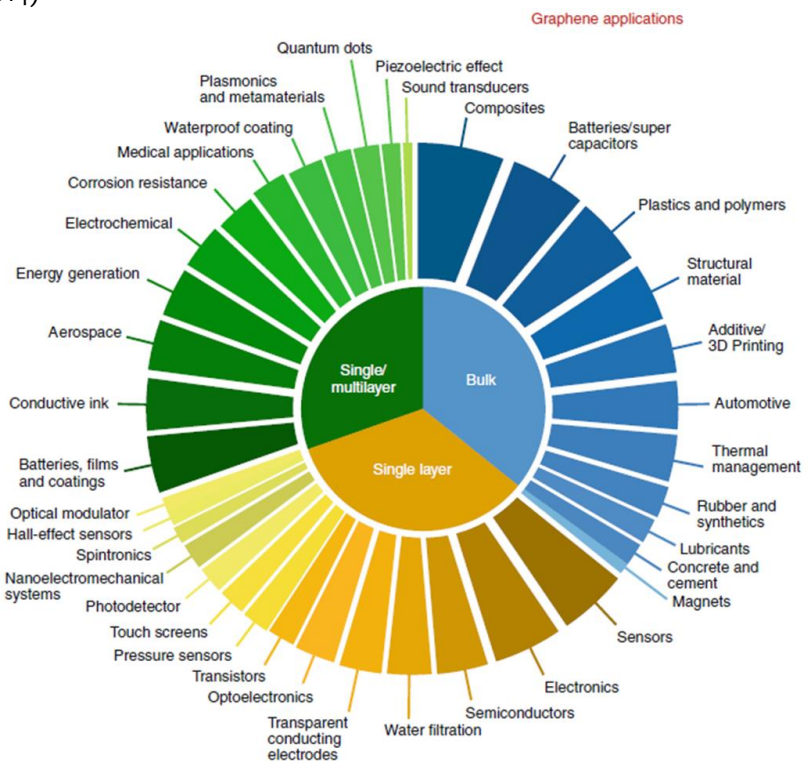

Figure 1.10: Applications of graphene in different fields. (Source: Barkan, 2019)

In the last 16 years, most of the research on graphene was done in academic institutions and newly developed start-ups with an aim to develop competitive commercial products. Various roadmaps have been designed to study the effect of this material on futuristic technology. However, there are several impediments to the commercial adoption of graphene. Some of the obstacles are inherently available in graphene itself, for example, lack of bandgap, making it unsuitable for switching applications. The other problems include a lack of standard grade graphene and expensive and complex characterization of the material. Despite all the setbacks, graphene has started registering its presence in the international commercial industry. Nowadays a large number of companies are producing graphene in large quantities, particularly in Europe and North America. A large number of graphene's applications have already been identified (Figure 1.10)(Barkan, 2019). For example, the addition of graphene to plastic and other composites improves their mechanical strength and electrical conductivity. An improvement of 30-40 % was observed in plastics by adding a very small amount of graphene (<1 %).

1.3 2D MATERIALS BEYOND GRAPHENE

In the last two decades,' graphene has been the show-stealer due to its exceptional properties. Since the isolation of graphene, various other 2D materials have also been explored for their wide range of applications in nano-electronic and photonic devices. Indeed, graphene is one of the most studied 2D material because of its exceptional properties, for instance, very high carrier mobility and electrical conductivity. However, graphene is not suitable for all applications, particularly for switching applications due to the absence of bandgap.

The success of graphene has triggered the researcher's interest to explore other 2D materials. Apart from graphene, several other 2D materials have also been discovered in recent years (Figure 1.11)(Bhimanapati et al., 2015). TMDs, hexagonal boron nitride, MXenes, and metal oxides are some of the typical examples of layered 2D materials exhibiting layered dependant properties as in case of graphene. These materials found more suitable than that of graphene, particularly for those applications where bandgap requirement is a prerequisite. For instance, by using TMDs for switching devices, a very high value of on/off ration can be achieved due to its sizeable bandgap(Radisavljevic et al., 2011).

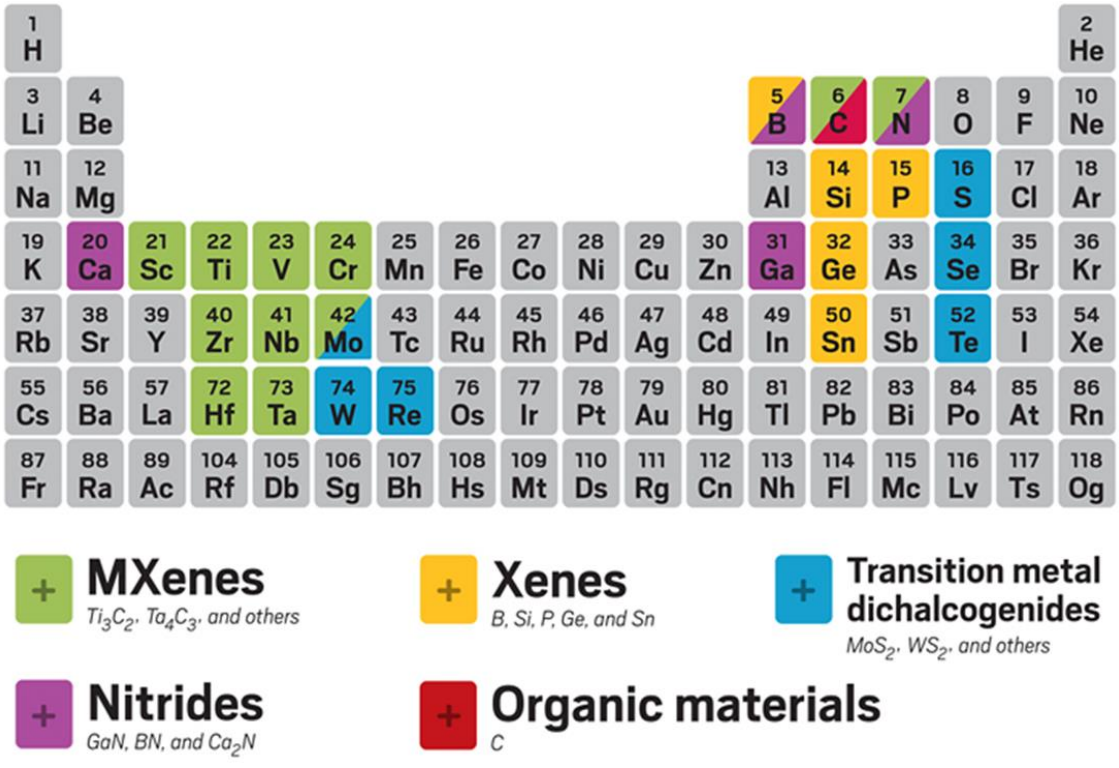

Figure 1.11: Different families of 2D materials beyond graphene. (Source: https://cen.acs.org/articles/95/i22/2-D-materials-beyond-graphene.html)

In the past few years, hexagonal boron nitride (BN) has shown its potential as a promising 2D layered dielectric material(Zhang et al., 2017). Due to its layered nature and structured similarity as that of graphene, it is also called "white graphene." This material has a wide bandgap of around 5.5 eV. In hexagonal BN, boron and nitrogen atoms are attached together in an alternating fashion. Similar to graphene, boron and nitrogen atoms are bonded together by strong covalent bonds within a layer. In contrast, the two different layers are held together by weak van der Waals interaction, as depicted in Figure 1.12. This weak van der Waals interaction allows the adjacent layers to be peeled off through the mechanical exfoliation method from bulk BN crystal. BN is transparent to electromagnetic waves and exhibit very high thermal conductivity. BN has been widely used for high-quality dielectric, atomically thin insulating material, and super thin tunneling applications.

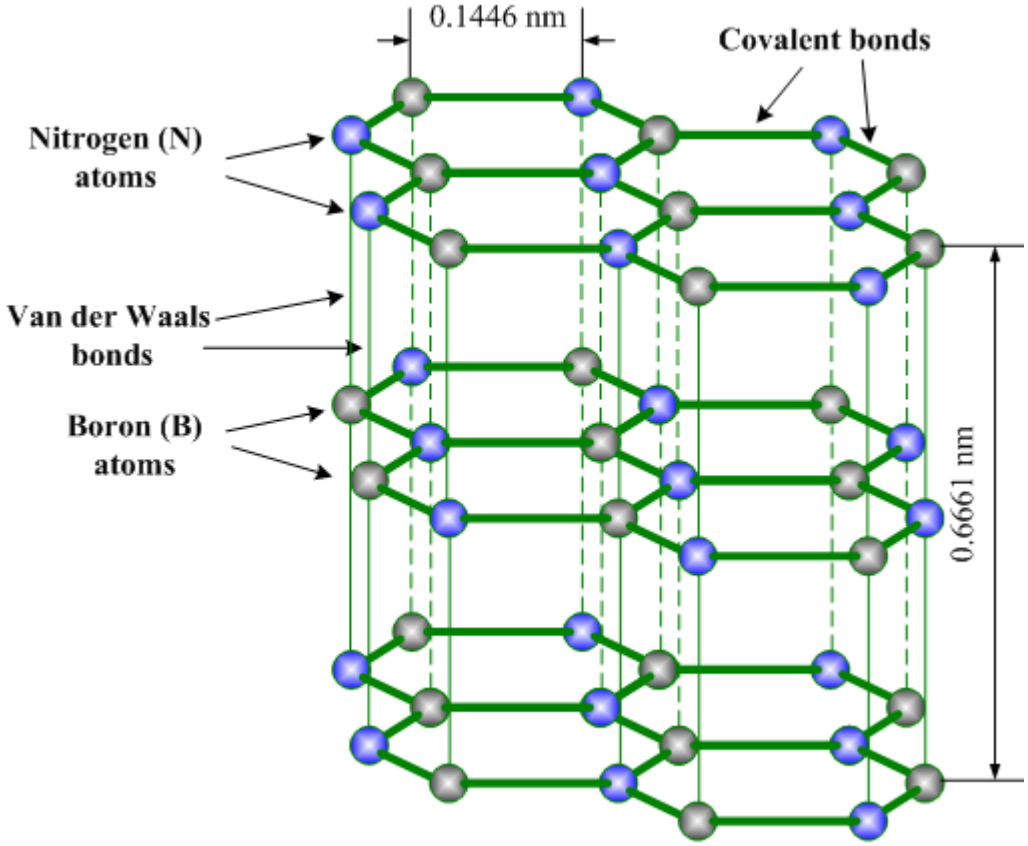

Figure 1.12: Schematic diagram of the hexagonal boron nitride crystal structure. (Source: https://www.substech.com/)

Phosphorene was discovered in 2014 through the mechanical exfoliation method from black phosphorus(Liu et al., 2014). It is also a layered 2D material like graphene and TMDs. Phosphorene grabs the researcher's interest due to its intrinsic tuneable direct bandgap and very large value of hole mobility. In single-layer phosphorene is having a bandgap of ~1 eV, while in its bulk form, the bandgap reduced to a value of 0.31 eV. In a few-layer phosphorene field-effect transistor, a high value of hole mobility (286 $cm^2/V.s$) and on/off ratio (10^4) was achieved. The side and top view of crystal structure phosphorene are shown in Figure 1.13.

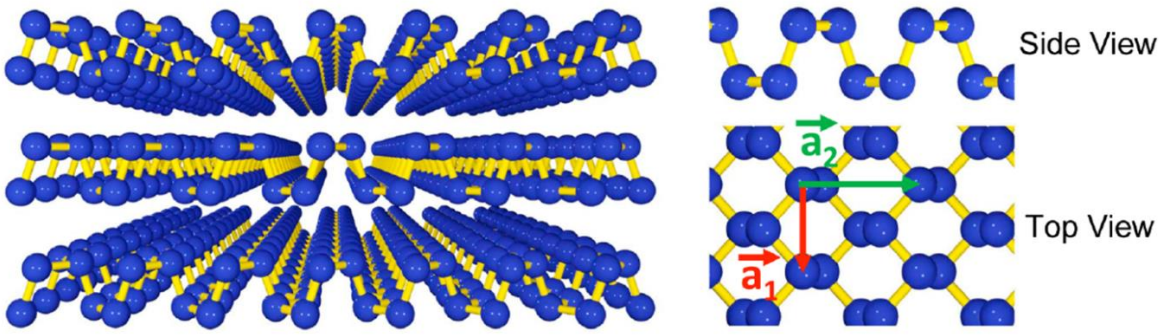

Figure 1.13: Side and top views of the crystal structure of few-layer phosphorene. (Source: Liu et al., 2014)

In the past three years, the carbides and nitrides of transition metals forming a popular family of 2D materials attracted huge research interest(Dhakal et al., 2015). This family is generally known as MXenes having formula $M_{n+1}AX_n$ (n= 1 to 3), where M is a transition metal belonging to d block of the periodic table, A is group IIIA or IVA element, and X is the caron and nitrogen. By changing the compositional ratio of M and X elements, the properties of MXenes can easily be tailored according to specific needs. After the first MXene compound ($Ti_3C_2T_x$) in 2011, approximately 40 MXenes compounds have been discovered so far. Crystal structures of MXenes having popular MAX phases are shown in Figure 1.14. These MXenes are primarily uses for energy storage devices, for instance, Li-ion battries, and electromical capacitors.

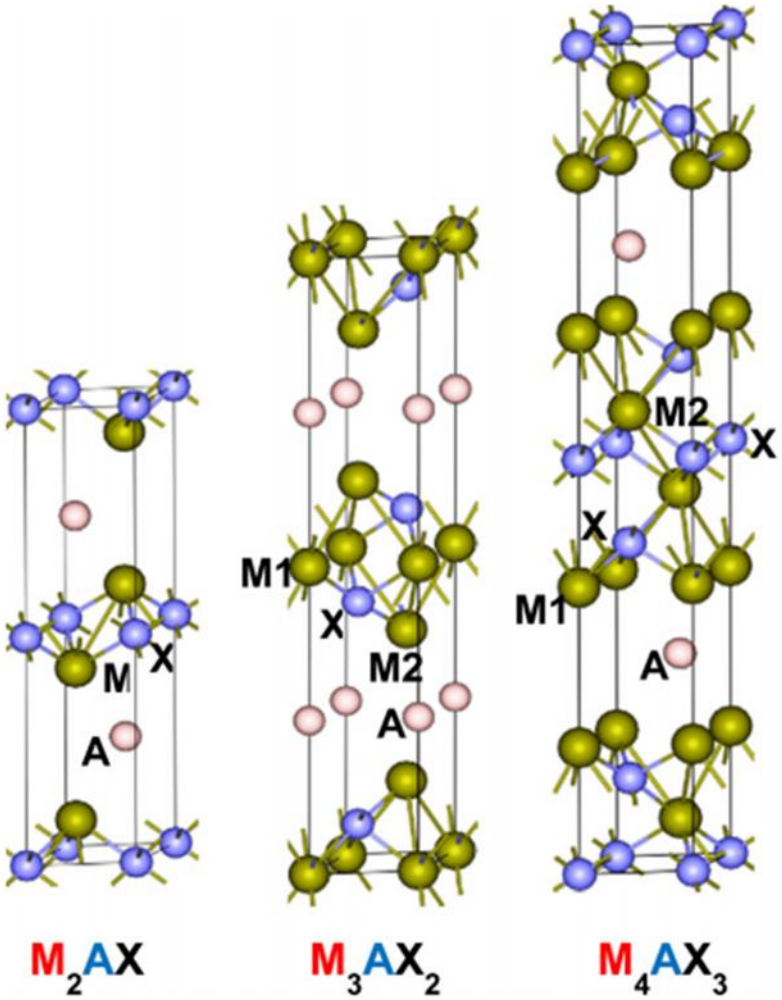

Figure 1.14: Schematic illustration of crystal structures of MAX phases. (Source: Dhakal et al., 2015)

The 2D materials discovered so far are just the tip of the iceberg, and a large number of 2D materials still need to be discovered with their exciting physics. With the large number of researchers involved in this field, several new 2D materials are found every year. For example, borophene is the newly discovered 2D material heaving single of boron atoms(Feng et al., 2016). Despite its short history, researchers have explored its potential for anode material for lithium-ion batteries and sensing material for sensing different gas molecules. Borophene characterization shows that it is more flexible and stronger than graphene. The schematic view of borophene is displayed in Figure 1.15. It possesses good electrical and thermal conductivity(Piazza et al., 2014). It is found suitable for its application in hydrogen and oxygen evolution reactions due to its excellent catalytic capabilities. However, borophene is prone to oxidation, which makes it difficult to handle. It should be protected carefully to avoid oxidation.

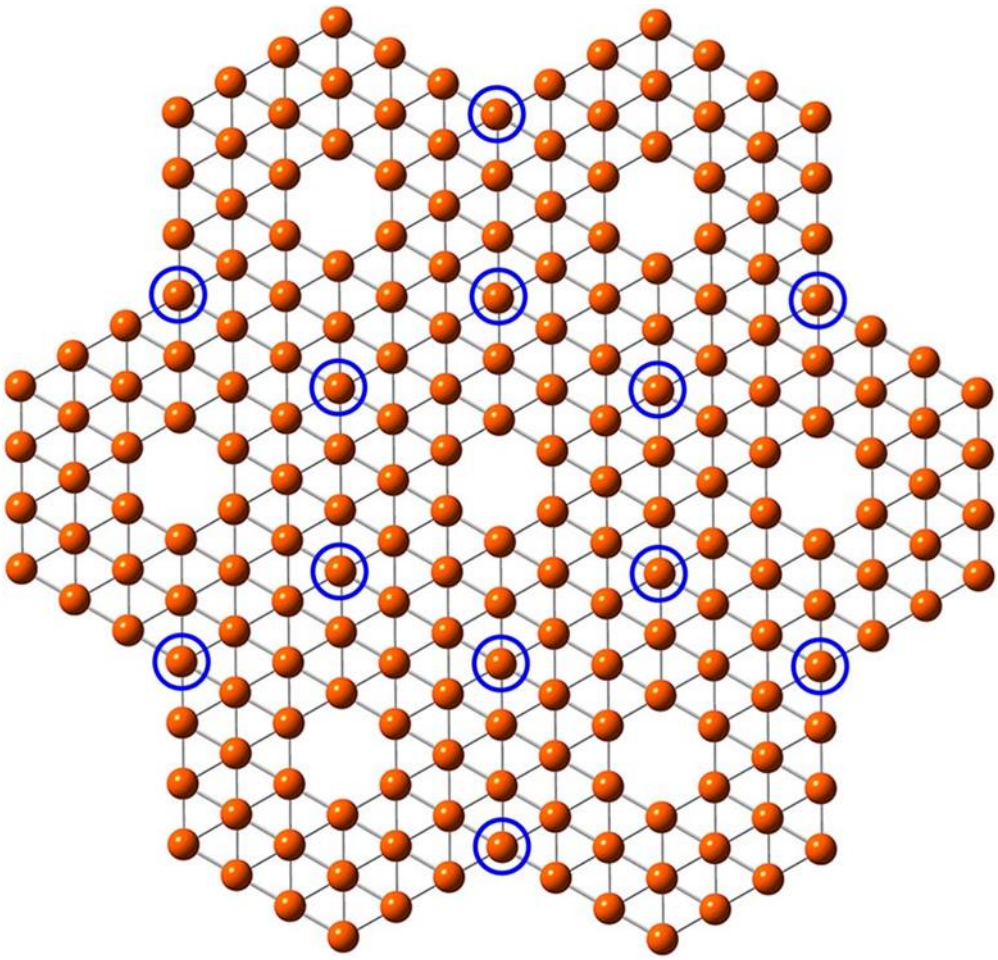

Figure 1.15: Schematic view of borophene. The blue circles represent the atoms shared by three units. (Source: Piazza et al., 2014)

It is predicted by the theoretical calculations, that most of the 2D materials possess excellent mechanical properties, a very high value of flexibility, and optical transparency. The transparency of these materials decreases with increasing the number of layers in 2D materials. The flexibility and transparency of these materials make them perfect candidates for next-generation foldable and wearable electronic and optoelectronic devices.

1.4 MOLYBDENUM DISULFIDE (MoS_2)

The other class of 2D materials is transition metal dichalcogenides (TMDs), heaving a sizeable bandgap, making them suitable for switching applications(Manzeli et al., 2017; Wang et al., 2012). These TMDs possess unique electrical, optical, chemical, and mechanical properties, these TMDs are found more suitable than graphene in some particular applications due to their tunable bandgap. Most of the TMDs have a strong in-plane covalent bond and weak van der Waals interlayer bonding. In TMDs, each layer is three atomic thick having MX_2 stoichiometry.

Here, M is a transition metal atom (M = Mo, W, Nb, Re, etc.), which is sandwiched between two chalcogen atoms (X = S, Se, Te), forming MX_2. Some of the popular combinations of MX_2 with their bandgap have been tabulated in Table 1.1. By choosing different combinations of M and X the phases and hence the electronic properties can be tuned.

The new functionalities of TMDs can be explored through phase engineering(Voiry et al., 2015). By choosing different arrangements of transition metal atoms and chalcogen atoms, their chemistry can be tailored for specific applications (Figure 1.16(a-e)). TMDs can occur in the trigonal prismatic phase (2H or 1H), depicting a hexagonal symmetry. In this configuration, different atoms are sequenced in ABA form, where A is the chalcogen atom, and B is the transition metal atom. The TMDs can also occur in the octahedral phase (1T), depicting tetragonal symmetry. In this case, the atoms sequenced in ABC form, due to change in the position of one sulfur atom compared to other atoms.

Table 1.1: Widely used combinations of MX_2 with their corresponding bandgap.

	-S2	-Se2	-Te2
Mo	Behaviour: Semiconductor Bandgap: 1.8- 1.2 eV	Behaviour: Semiconductor Bandgap: 1.5- 1.1eV	Behaviour: Semiconductor Bandgap: 1.1- 1.0 eV
W	Behavior: Semiconductor Bandgap: 2.1- 1.4 eV	Behavior: Semiconductor Bandgap: 1.7- 1.2 eV	Behavior: Semiconductor Bandgap: 1.1 eV
Nb	Behavior: Superconducting	Behavior: Superconducting	Metallic

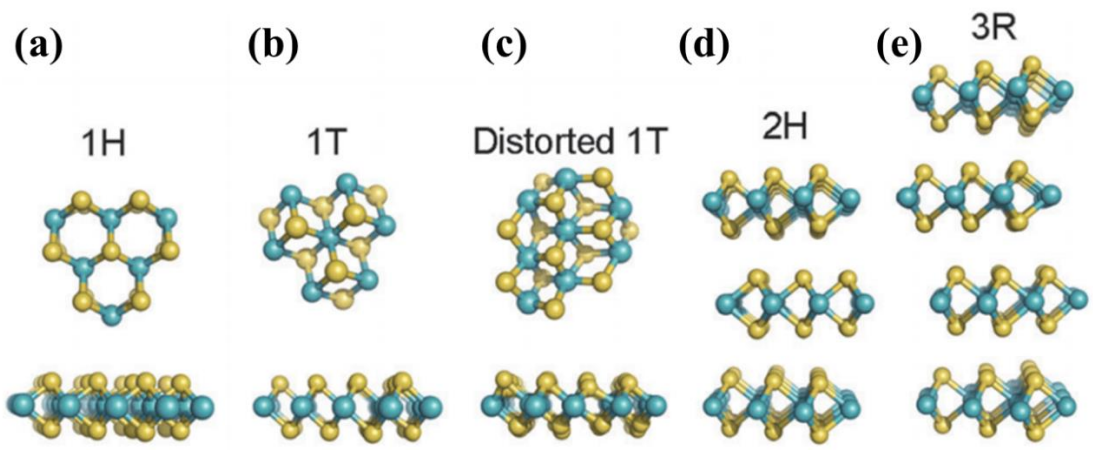

Figure 1.16: Different phases of TMDs due to different stacking positions of transition metal and chalcogen atoms. (a) 1H, (b) 1T, (c) distorted 1T, (d) 2H, and (e) 3R phases. (Source: Voiry et al., 2015)

Over the last decade, MoS_2 is one of the most studied 2D layered material which belongs to the family of TMDs(Ganatra and Zhang, 2014). It has proved its significant potential for a wide range of applications. The exciting physics of three atomic thick layer of MoS_2 gives new insights in the field of low dimensional materials. MoS_2 possesses a tunable bandgap of 1-2 eV and a high value of electron mobility. One of the silent features of MoS_2 is its existence in different crystal structures. MoS_2 has the capability to form 2H, 3R, 1T, and 1T' crystal structures, as shown in Figure 1.16. Each MoS_2 layer is three atomic thick having a thickness of 6.5 A˚, as shown in Figure 1.17(Radisavljevic et al., 2011). Transition metal d-orbital filling

decides the electronic structure of MoS_2 rather than the s- and p- orbitals hybridizations. The semiconducting behavior in MoS_2 occurs due to complete filled d- orbitals, while the metallic behavior arises due to partially filled d-orbitals(Jiang et al., 2015). The trigonal phase or octahedral phase of MoS_2 also depends on the partial or complete filling of d- orbitals. For example, the presence of 0 electrons in the d- orbital results in the trigonal prismatic phase, while the presence of 6 electrons in the d- orbital (completely filled) ensures the octahedral phase. MoS_2 possesses unique bandgap tunability from indirect to direct bandgap, few atoms thin thickness, strong spin-orbital coupling, and promising electronic and optoelectronic properties. Due to these qualities, MoS_2 find application in high performance electronic and optoelectronic devices, flexible and wearable electronic devices, and energy storage devices(Li et al., 2014).

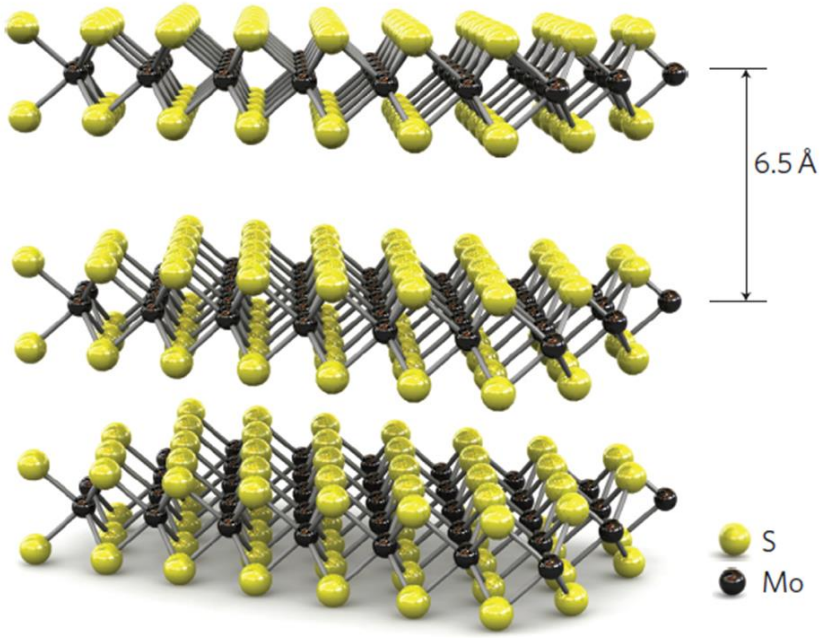

Figure 1.17: The 3D schematic illustration of the crystal structure of MoS_2. Each layer of MoS_2 is 6.5 A˚ thick. (Source: Radisavljevic et al., 2011)

In the last seven years, MoS_2 dominants the number of publications in the field of optoelectronics, as shown in Figure 1.18. Most of the reports are published on MoS_2, black phosphorus (BP), and heterostructures (HS) using different materials(Thakar and Lodha, 2020). However, the practical application of black phosphorus is questionable due to its environmental instability. The first monolayer MoS_2 transistor was demonstrated experimentally by Radisavljevic et al., as shown in Figure 1.19(a)(Radisavljevic et al., 2011). Monolayer MoS_2 (6.5 A˚) works as the semiconducting channel. The single-layer MoS_2 was exfoliated on SiO_2/Si substrate by mechanical exfoliation technique. The AFM image and corresponding height profile of exfoliated MoS_2 flake is shown in Figure 1.19(b and c). They have used hafnium oxide as a gate dielectric to increase the mobility of charge carriers in a monolayer MoS_2 to a value of 200 cm^2/Vs. The high value of mobility was achieved due to the dielectric screening effect. In addition to very high mobility, they have obtained a very large value of the current on/off ratio of the order of 10^8, as shown in Fig 1.19(d). The very high value of on/off ratio result in ultralow power consumption. Here, HfO_2 is used as a gate dielectric due to its very large value of dielectric constant (€=25) and a higher value of bandgap (E_g = 5.7 eV). The top gate controls the output current of the transistor very efficiently, as shown in Figure 1.19(e).

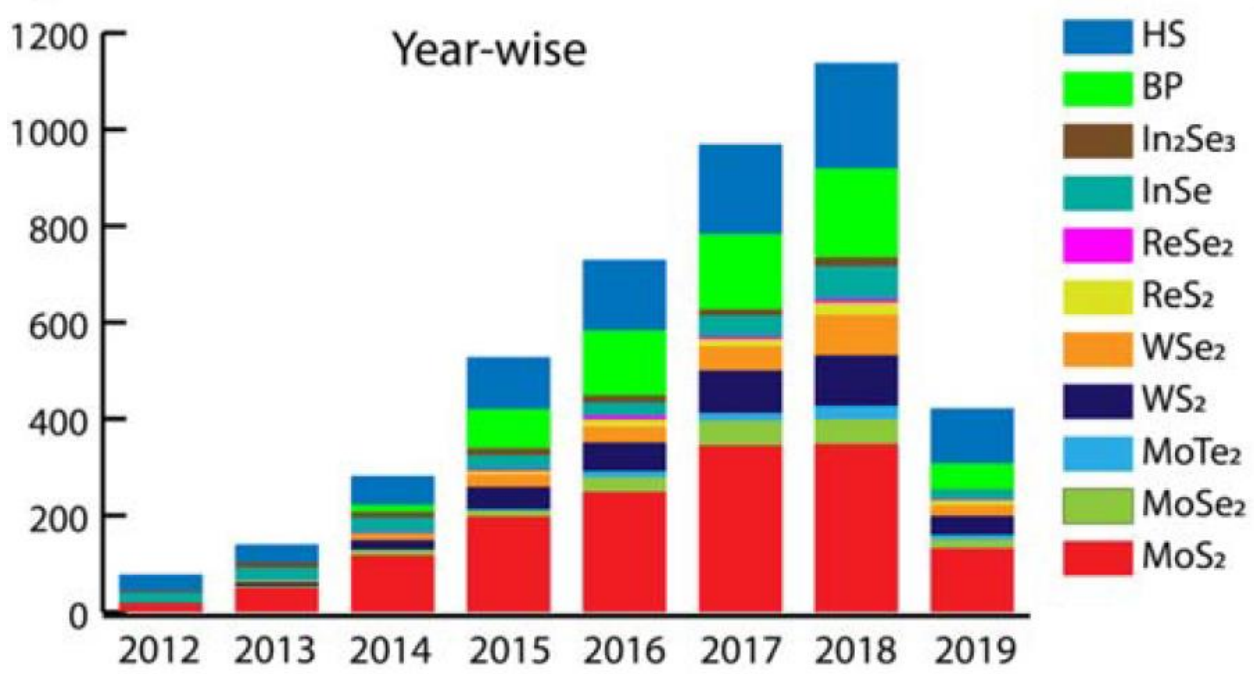

Figure 1.18: Year-wise number of publications in the field of optoelectronics for most widely used 2D materials. (Source: Thakar et al., 2020)

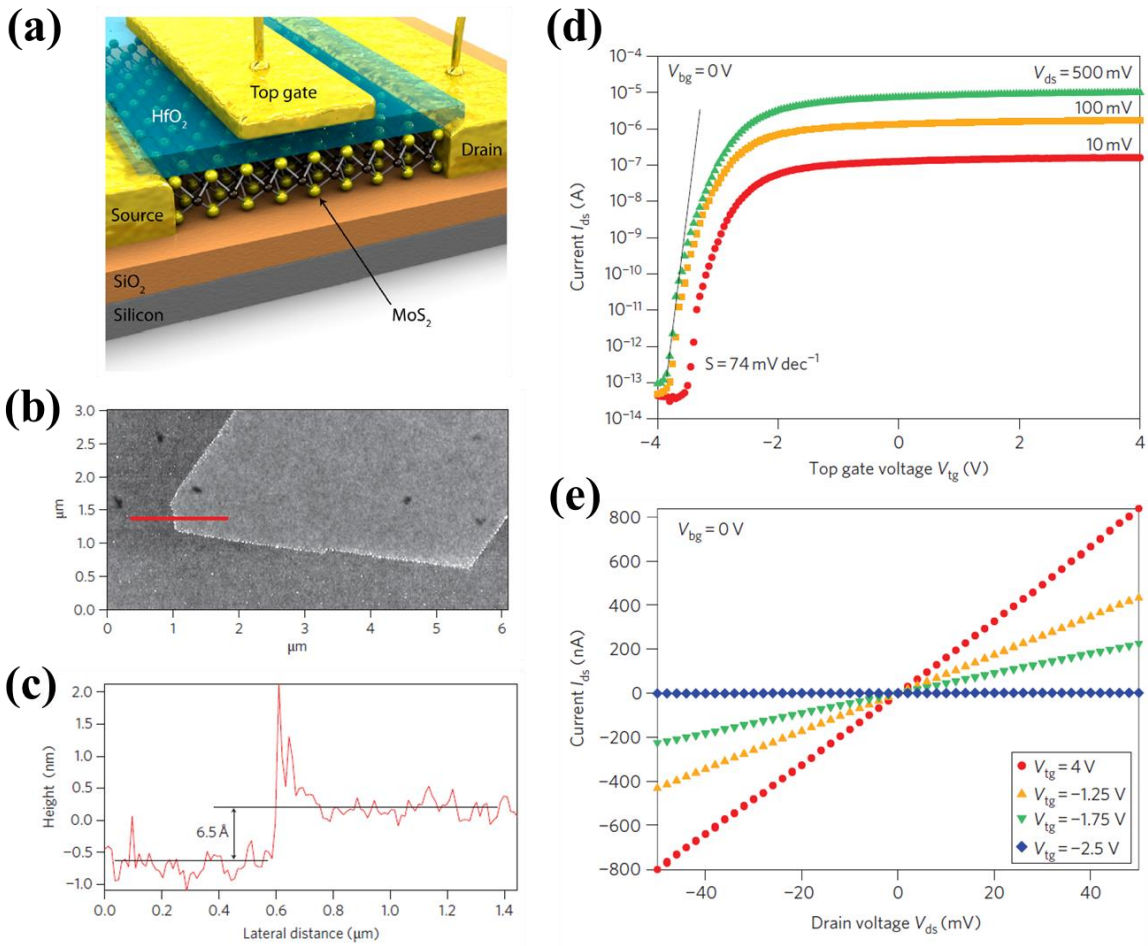

Figure 1.19: (a) Schematic illustration of monolayer MoS_2 based transistor. (b) AFM image and (c) height profile along the solid red line of mechanically exfoliated MoS_2 flake on SiO_2/Si substrate. (d) The Transfer characteristics depicting a very high value of on/off ratio (> 10^8) for V_{ds} = 500 mV. (e) Output characteristics at different top gate voltage. (Source: Radisavljevic et al., 2011)

MoS_2 has also shown its promising behavior in optoelectronic applications due to its high value of the absorption coefficient. Lopez-Sanchez et al. have demonstrated a MoS_2 phototransistor as shown in Figure 1.20(a)(Lopez-Sanchez et al., 2013). The optical image of phototrasistor based on MoS_2 flake is depicted in Figure 1.20(b). They observed a photoresponsivity as high as 880 A/W at 561 nm (Figure 1.20(c)). This high value of photoresponsivity was achieved due to improved mobility and high-quality contact formation. The I-V characterization of the device under different light irradiation intensities at a wavelength of 561 nm is shown in Fig 1.20(d). A manifold increase in the drain current was obtained with increase in intensity of light irradiation.

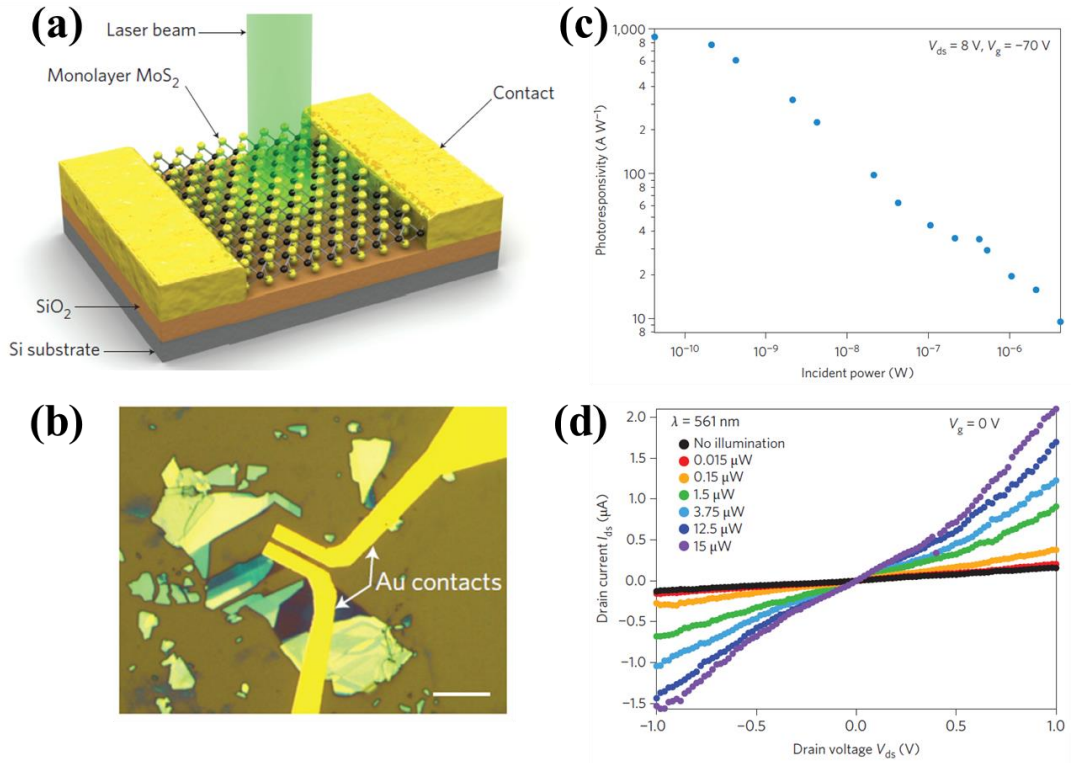

Figure 1.20: (a) 3D schematic illustration of ultrasensitive MoS_2 photodetector. (b) Optical image of MoS_2 based transistor. (c) Photo-responsivity of the device depicting a value as high as 880 A/W under light irradiation of 150 pW. (d) Output characteristics of the device in the dark and under various light irradiation intensities. (Source: Lopez-Sanchez et al., 2013)

In recent years, few-layer MoS_2 has also established itself as a promising material for various applications. The few-layer MoS_2 offers a higher density of states, a higher value of mobility, a lower value of interface scattering, and a lower value of contact resistance. In 2013, Late et al. have studied the sensing performance of single- and few-layer MoS_2 upon exposure to NO_2 and NH_3 (Late et al., 2013), as shown in Figure 1.21 (a and b). After comparing the results from both types of devices, it was observed that few-layer MoS_2 is more suitable for sensing applications due to its excellent sensing response and recovery. The improvement in sensing response of few-layer MoS_2 is due to its different electronics structure and more stable response over time.

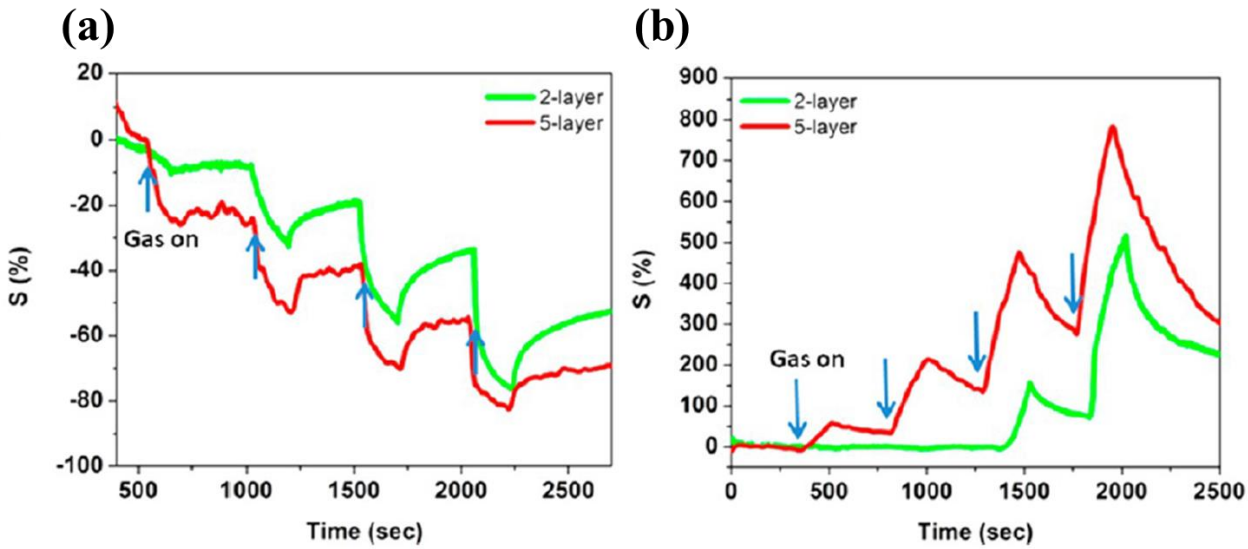

Figure 1.21: Comparison of sensing ability of 2- and 5- layer MoS_2 film upon exposure of varying concentration of (a) NH_3 and (b) NO_2. (Source: Late et al., 2013)

Due to the versatility of MoS_2, sensors with multifunctional applications have also been developed. A bi-functional sensor has been synthesized by Cho et al. using chemical vapor deposited MoS_2 as displayed in Figure 1.22(a)(Cho et al., 2015). For evaluating the gas sensing behavior of the sensor, the device was exposed to NO_2 gas molecules. NO_2 extracts the electrons from the MoS_2 surface resulting in an increase in resistance. Therefore, an increase in NO_2 concentration lead to an increment in resistance and hence the sensitivity (relative change in resistance), as shown in Figure 1.22(b). The sensitivity of the device increases linearly with an increase in NO_2 concentration, as shown in Figure 1.22 (c). A detection limit of 120 ppb was achieved using this MoS_2 based sensor. At room temperature, complete recovery is not possible due to the poor desorption rate of gas molecules. Thus, thermal energy is provided to improve the recovery of the device, as shown in Figure 1.22(d). However, increasing temperature also decreases the device sensitivity. To evaluate the stability and practicality of the sensor, a cyclic test was performed upon 120 ppb NO_2 exposure, as displayed in Figure 1.22(e). The cyclic test confirms the stability of the fabricated device. To measure the selectivity of the sensor, the sensitivity of the device against different gas molecules was compared. Figure 1.22(f) clearly indicates that the device was highly selective towards NO_2. NO_2 could also be detected even when mixed with other atmospheric gases (inset of Figure 1.22(f)), making the device a perfect candidate for real environment monitoring applications. The same device also shows a reliable photosensitivity behavior with a photoresponsivity of ~ 71 mA/W and photoresponse < 500 ms. The multifunctional sensing behavior paves the way for efficient, futuristic electronic devices.

Our group has also exposed the potential of multilayer MoS_2 based gas sensors for ultrafast detection of NO_2 gas(Kumar et al., 2017). Interestingly, we have developed a NO_2 gas sensor that works at room temperature, unlike the previously available high temperature operated sensors. Due to the absence of a heating element, our sensors offer some distinct features such as ultra-low power consumption, portable, and very low cost. This milestone was achieved by using ultraviolet (UV) light, resulting in dramatically high sensitivity coupled with an ultrafast response time and excellent recovery. Photoexcited charge carriers generated under the UV illumination reacts with atmospheric oxygen, and humidity present on the MoS_2 surface forms O_2 (gas) and leaves the MoS_2 surface. Thus under UV illumination, the surface of MoS_2 got cleaned and became more responsive by exposing a higher number of reactive sites that were previously unavailable. Upon exposure of NO_2, more number of electrons got extracted from cleaned MoS_2 surface resulting in a large change in MoS_2 resistance and, eventually, high sensitivity at room temperature.

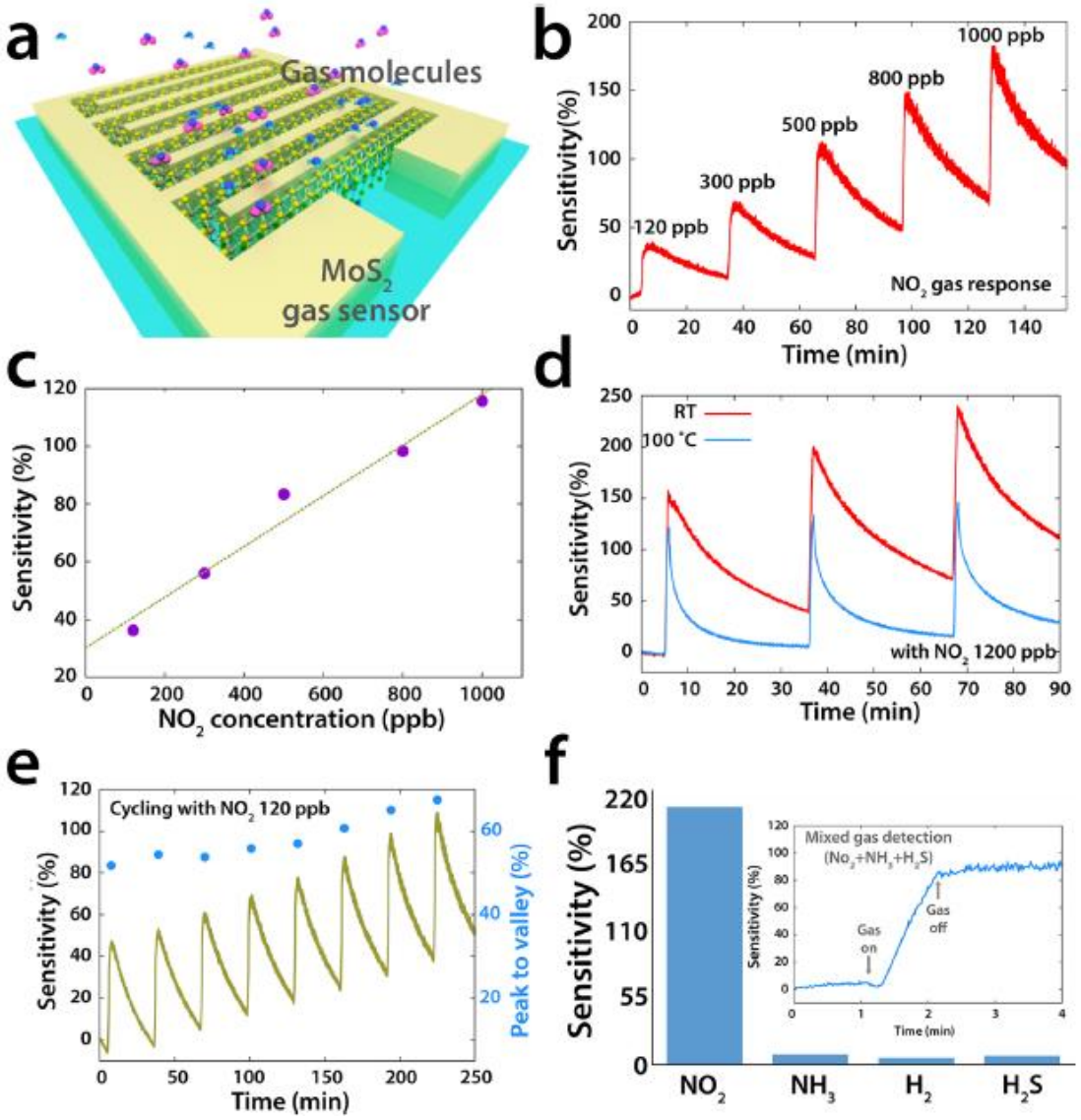

Figure 1.22: (a) Schematic representation of MoS_2 based gas sensor. (b) The sensitivity of the device with varying concentrations of NO_2 at room temperature. (c) A liner fitting of between sensitivity and different concentrations of NO_2 using Langmuir's model. (d) Comparison of sensing performance of the device at room temperature and 100 ˚C. (e) Cycling text at 120 ppb NO_2 concentration to evaluate the stability of the device. (f) The selectivity of the device to different gas analytes. The inset shows the sensing response under mixed gas environment. (Source: Cho et al., 2015)

1.5 HETEROSTRUCTURES

The integration of different dimensional materials with 2D materials to form heterojunctions for efficient photo and gas sensing applications has attracted worldwide efforts. In these kinds of heterojunctions, the conventional constraints of lattice matching are relaxed, and a higher value of surface sensitivity is achieved. These heterojunctions also offer a higher degree of controllability and tunability with improved device features. Moreover, in these heterojunctions based sensors, even a small change in barrier height or depletion width at the heterointerface results in a very large change in resistance, and hence excellent sensing response was achieved. The limitations of individual materials can easily be overcome by forming heterojunctions. Considering the particular advantages of individual materials, a hybrid approach could be more effective in dealing with the current sensing challenges.

A heterostructure is formed when two different bandgap semiconductors shared a common interface. By controlling the valance band and conduction band offsets, these heterostructures can easily be tuned for a specific application. Over the last decades, these

heterostructures can be used for many interesting applications. A discontinuity occurs at the heterointerface due to differences in the wok function of the constituent semiconductors. In general, the presence of discontinuity can broadly be classified into three groups, as depicted in Figure 1.23(Sze and Ng, 2006).

(a) Type-I (straddling)
(b) Type-II (staggered)
(c) Type-III (broken gap)

Depending upon a particular type, these heterostructure have their particular function. For instance, type-I and type-II heterostructures are mostly used for optoelectronic devices(Özcelik et al., 2016). The strong carrier confinement allows efficient recombination of generated charge carriers.

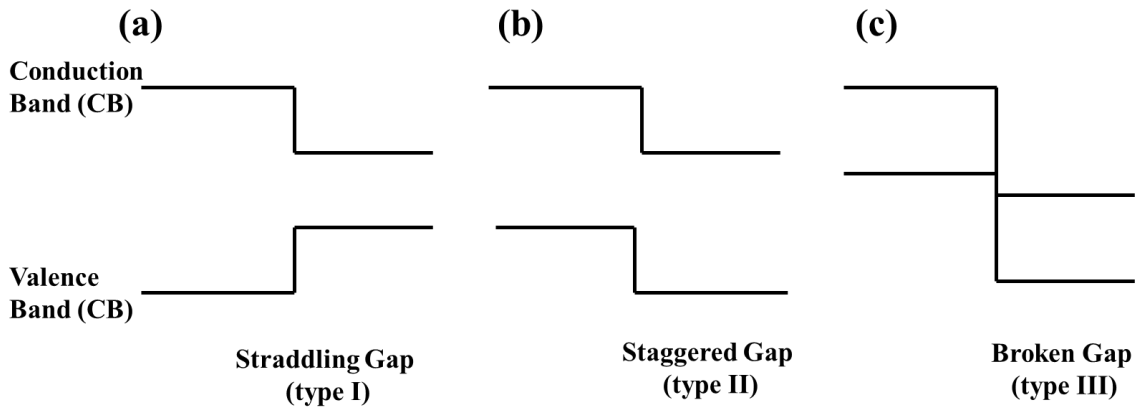

Figure 1.23: Different kinds of band alignments at the heterointerfaces.

Different materials have their distinct properties applicable to a specific application, as shown in Figure 1.24(a). Over the last decade, numerous efforts have been made to tune the properties of 2D materials by using several techniques. Few of these efforts include integrating different dimensional materials to form heterostructures, phase engineering 2D materials, and functionalizing the 2D materials through noble metal particles. Among all these existing techniques, multifunctional heterostructures formed by combining different dimensional materials are most popular, as shown in Figure 1.24(b-f)(Liu et al., 2016). By combining different materials together, a new class of materials emerges, finding its applicability in diverse applications. These heterostructures find their applications in the field of electronics, optoelectronics, energy storage, gas sensing, and biomedical engineering.

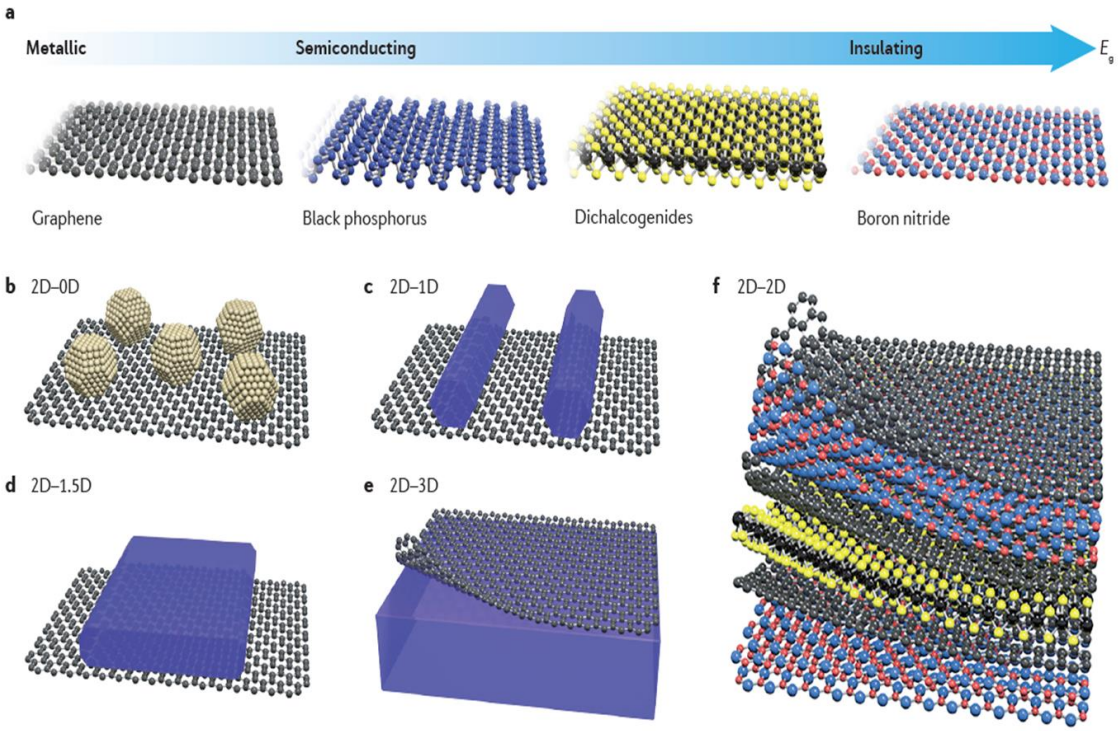

Figure 1.24: (a) The classification of 2D materials based on their properties. (b-f) multifunctional heterostructures formed by combining different dimensional materials. (Source: Liu et al., 2016)

1.6 APPLICATIONS OF HETEROSTRUCTURES

Several efforts have been made to understand the device physics after combining 2D materials with other 2D or non-2D materials. Although, the heterostructures with at least one 2D material are more popular than any other combination. In those kinds of heterostructures, the conventional constraints of lattice matching are relaxed(Jariwala et al., 2017). A higher degree of controllability and tuneability was observed with improved device features after forming heterostructures. Moreover, the applied gate voltage tuneability provides an extra degree of freedom to modulate the interface at the heterojunction. In this section, we have explained the uses of 2D based heterostructures, particularly in the field of photo and gas sensing applications.

1.6.1 Applications of 0D/2D heterostructures

The 0D materials mainly include quantum dots, nanoparticles, and tiny organic molecules, as shown in Figure 1.25(Jariwala et al., 2017). These 0D/2D heterostructures are widely used for broad-spectrum photo-sensing applications. These heterostructures also enhance the gas sensing performance of the devices by creating fresh active sites for gases to get adsorbed and by multiple nonojunctions at the surfaces. The sensing mechanism of such devices depends on the charge transfer at the heterointerfaces.

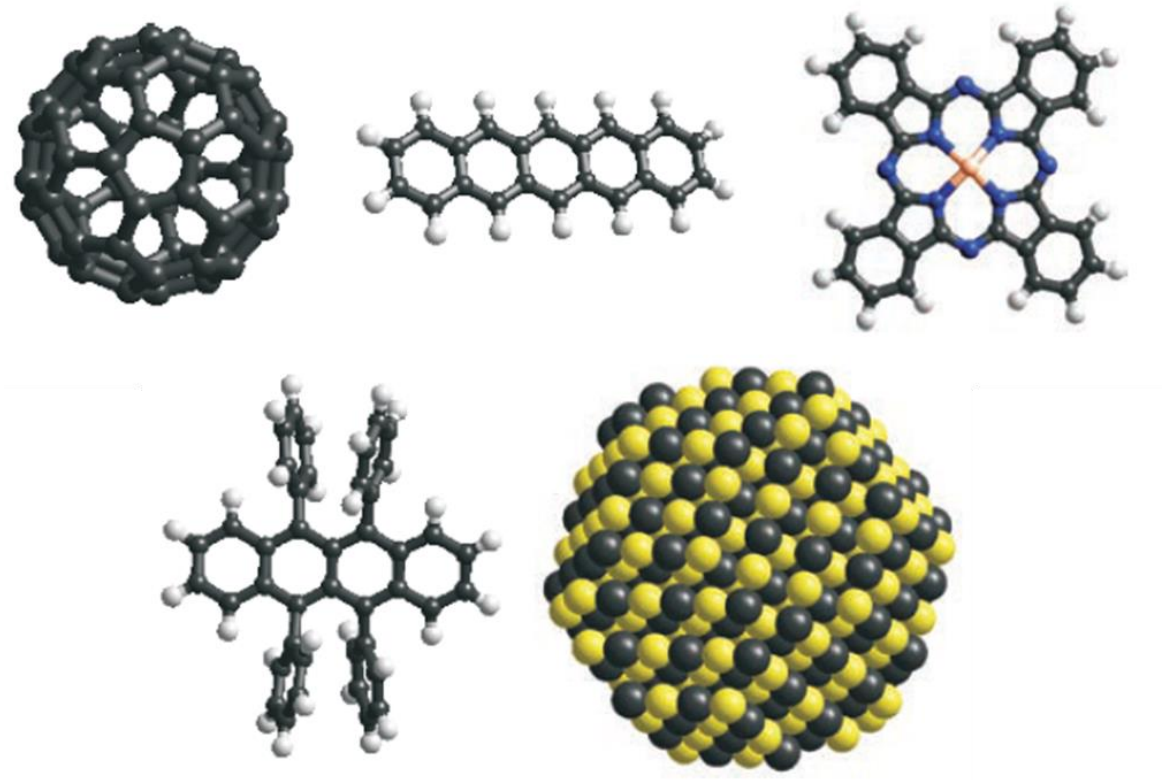

Figure 1.25: Schematic illustration of 0D materials, including fullerenes, tiny organic molecules, and quantum dots. (Source: Jariwala et al., 2016)

A 0D/2D heterostructure based photodetector comprising of MoS_2 and graphene quantum dots is demonstrated by Chen et al.(Chen et al., 2015). The schematic representation of the fabricated device is shown in Figure 1.26(a). The MoS_2 film was grown by atmospheric pressure chemical vapor deposition technique, while graphene quantum dots were fabricating by microwave-assisted hydrothermal process. Due to trapping of photoexcited charge carriers at the heterointerface, carrier lifetime, and hence the photoresponsivity and photogain increases. A five-time improvement in drain current and photocurrent of the heterostructure based device then that of only MoS_2 based device has been observed as shown in Figure 1.26(b and c). Due to the large value of photocurrent, a higher degree of gate tenability was also observed in the MoS_2-graphene quantum dot based device. A responsivity of the order of 4 was calculated, which is significantly higher than pure MoS_2 based devices (Figure 1.26(d)). The photoresponsivity decreases exponentially, which increases in light intensities.

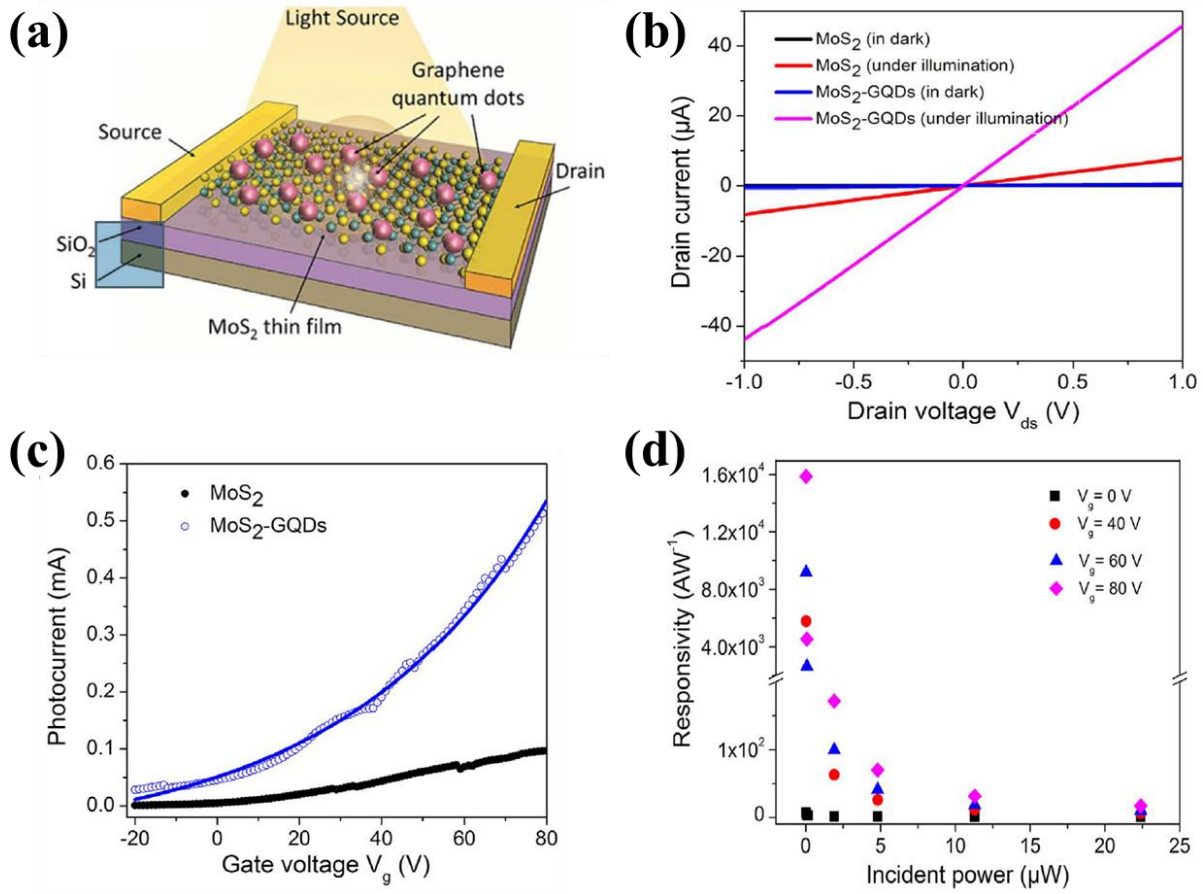

Figure 1.26: (a) Schematic illustration of the MoS_2-graphene quantum dots based photodetector. (b) I_{ds}-V_{ds} characteristics of in presence and absence of 405 nm light irradiation for the only MoS_2 and MoS_2-graphene quantum dots based photodetector. (c) Gate tenability of photocurrent. (d) Photoresponsivity as a function of incident optical irradiation. (Source: Chen et al., 2015)

Kufer et al. have also demonstrated a 0D/2D heterostructure based photodetector comprising of 0D PbS quantum dots and 2D MoS_2 few-layer thick film(Kufer et al., 2015). The band alignment at PbS/MoS_2 heterointerface is shown in Figure 1.27(a). The photoinduced charge carriers get separated at the heterointerface. The current flow across the device can easily be controlled by controlling the gate voltage. With an increase in light irradiation intensity, the built-in potential at the heterointerface decreases, resulting in a lower value of photoresponsivity. Figure 1.27(b) compared the photoresponsivity of only MoS_2 film and MoS_2/PbS hybrids. Several orders of higher photoresponsivity were observed in a hybrid structure.

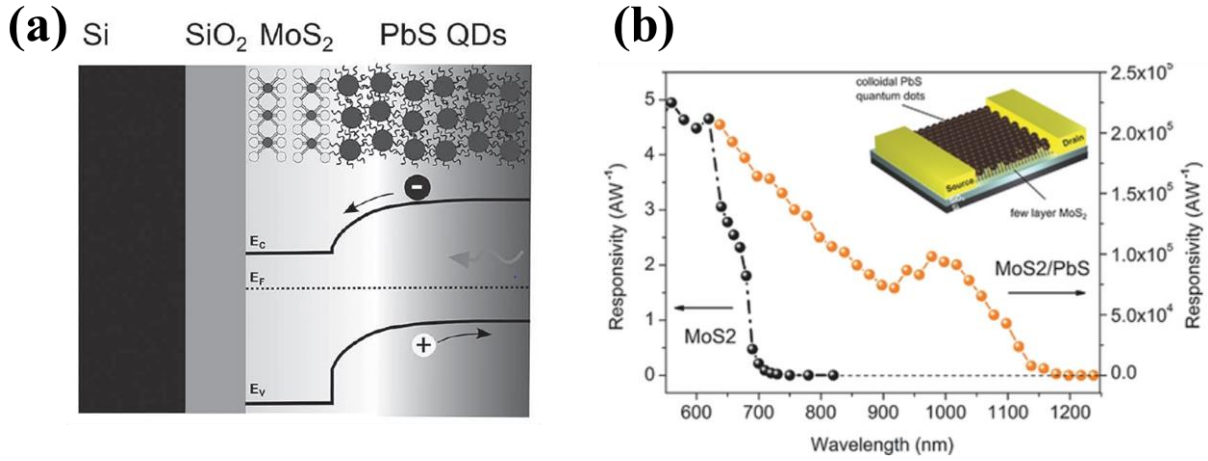

Figure 1.27: (a) Band alignment at the MoS_2/PbS heterointerface. The photoinduced charge carriers get separated at the interface. (b) Comparison of photoresponsivity of only MoS_2 film and MoS_2/PbS hybrids. The inset shows the schematic representation of the MoS_2/PbS hybrid device. (Source: Kufer et al., 2015)

0D/2D heterostructures are not limited to only photo sensing applications, these heterostructures have also registered their strong presence in the field of gas sensing applications. Qin et al. have demonstrated a 0D/2D heterostructure for gas sensing applications(Qin et al., 2017). They decorated TiO_2 quantum dots on WS_2 nano-sheets for NH_3 sensing. The number of adsorption sites for gas molecules increases significantly after decorating TiO_2 quantum dots. Therefore, a 17 times improvement in sensing has been recorded. Moreover, the efficient electron transfers from WS_2 to TiO_2 (Figure 1.28(a)) form a large number of depletion regions at the heterointerfaces (Figure 1.28(b)). Thus, a large change in current was observed due to reducing depletion width after exposing NH_3 gas into the chamber, as shown in Figure 1.28(c).

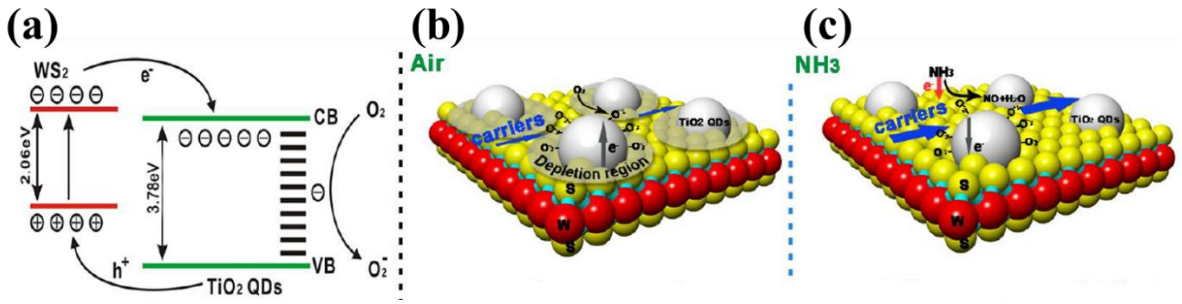

Figure 1.28: (a) Energy band diagram at the TiO_2/WS_2 heterointerface. Schematic illustration of TiO_2/WS_2 nanohybrids in (b) air and (c) NH_3 molecules. (Source: Qin et al., 2017)

Similarly, a 0D/2D heterostructure for efficient hydrogen detection at room temperature was also demonstrated by Kuru et al.(Kuru et al., 2015). A Pd-MoS_2 nanocomposite was fabricated by the solution-processed method. Figure 1.29(a) and 1.29(b) displays the optical image and SEM image of the device, respectively. This method involves drop-casting of MoS_2-$PdCl_2$ solution on the substrate followed by an annealing process. The sensing response of Pd-MoS_2 nanocomposite upon hydrogen exposure is shown in Figure 1.29(c). A very high value of sensitivity and the fast response was achieved due to the modulation of the work function of Pd nanoparticles. This modulation in work function is due to the formation of palladium hydrides upon hydrogen exposure. The sensing performance of the composite with varying concentration of hydrogen is shown in Figure 1.29(d). The sensor shows complete recovery at room temperature without any external stimulus. The sensing performance of Pd-MoS_2 hybrid is much batter then pristine MoS_2 based sensors.

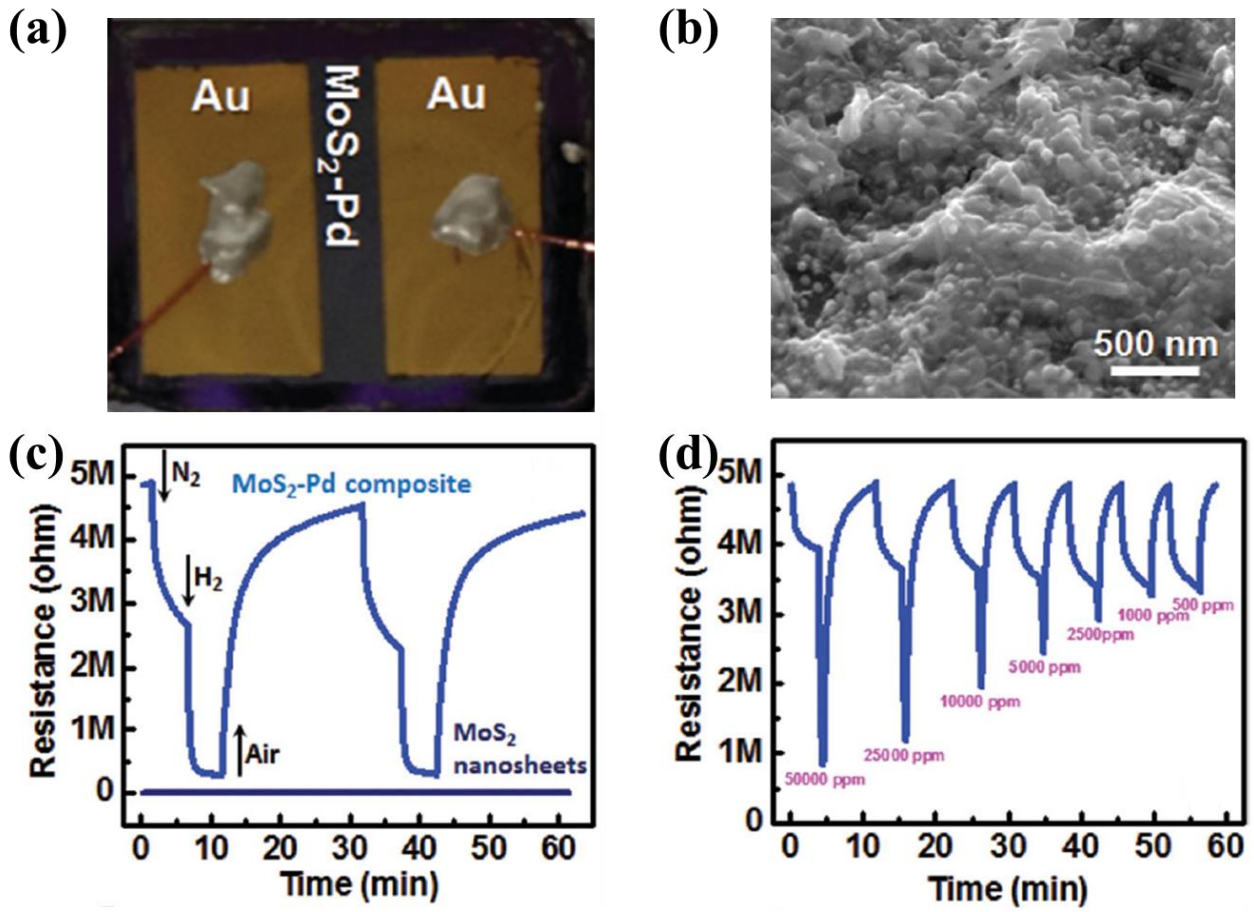

Figure 1.29: (a) Photograph of Pd-MoS_2 nanocomposite sensing device. (b) SEM image of Pd-MoS_2 hybrids. (c) Sensing response of pristine MoS_2 and Pd-MoS_2 hybrid upon exposure to hydrogen. (d) Sensing response of Pd-MoS_2 hybrids upon exposure to different concentrations of hydrogen. (Source: Kuru et al., 2015)

1.6.2 Applications of 1D/2D heterostructures

The discovery of carbon nanotubes in 1990 opened a new era of 1D materials in the electronic industry. Several types of 1D structures, including nanowires, nanoribbons, nanorods, polymeric chains, have been extensively studied due to their exciting physics for promising technological applications (Figure 1.30). These 1D nanostructures play a crucial role in developing next-generation electronic and optoelectronic devices(Jariwala et al., 2017). Some physical phenomenon such as quantum mechanical effects becomes more dominating in these kinds of nanostructures due to their small diameter. Moreover, the inherent large surface to volume ratio of these 1D nanostructures is widely used for different sensing applications. In recent years, these 1D nanostructures were combined with 2D materials to increase light absorption in photodetectors. These 1D/2D heterostructures are also useful for gas sensing applications because of increased adsorption of gas analytes.

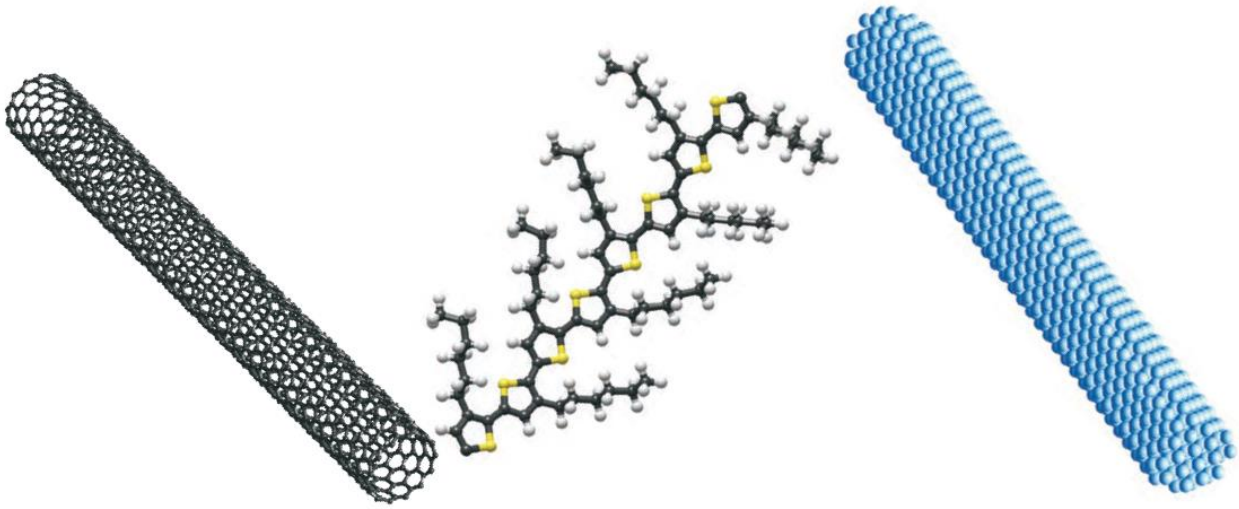

Figure 1.30: Schematic illustration of 1D structures, including carbon nanotube, polymers, and Si nanowire. (Source: Jariwala et al., 2016)

A gate modulated 1D/2D heterostructure using carbon nanotube, and monolayer MoS_2 was demonstrated by Jariwala et al., as shown in Figure 1.31(a)(Jariwala et al., 2013). A current on/off ratio of more than 10^4 was achieved at the heterointerface. The gate modulated values of photocurrent at different wavelengths under reverse bias conditions are shown in Figure 1.31(b). With increasing negative gate voltage, the depletion region extends deeper into the MoS_2, leading to a lower value of photocurrent. The carbon nanotube/MoS_2 heterostructure possesses an appealing photo sensing performance with an ultrafast response of less than 15 μs and a quantum efficiency of 25%.

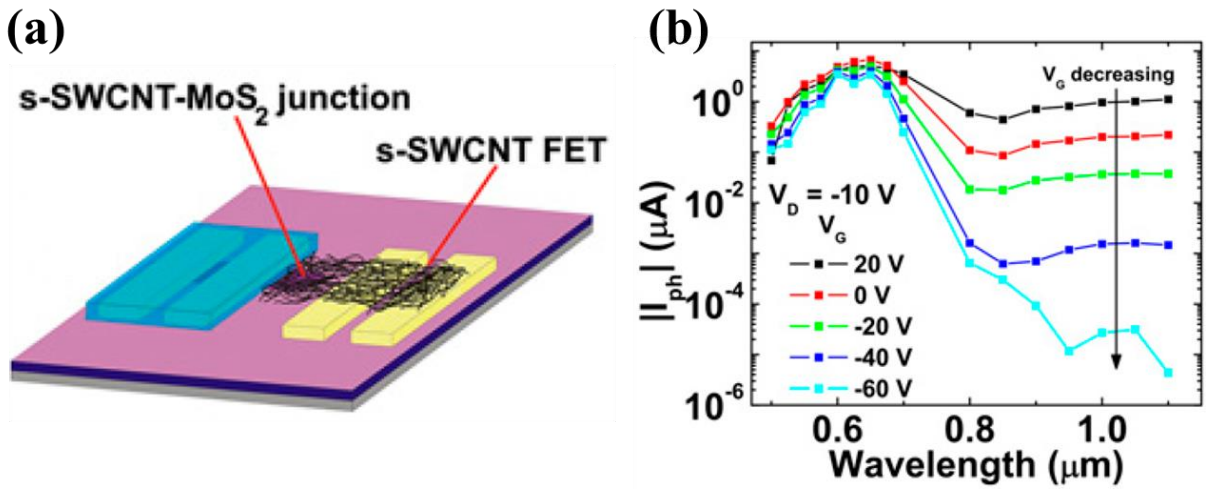

Figure 1.31: (a) Schematic representation of single-walled carbon nanotube/MoS_2 heterostructure. (b) Gate modulated photocurrent at different wavelengths. (Source: Jariwala et al., 2013)

MoS_2/carbon nanotubes hybrids not only used for photo sensing applications but for gas sensing applications also. Deokar et al. have demonstrated the excellent sensing ability of carbon nanotubes functionalized with MoS_2 nanoplates(Deokar et al., 2017). The hybrid structure was synthesized using a conventional CVD technique. The response and recovery curves of the device against varying concentrations of NO_2 are shown in Figure 1.32(a). The response curve of the device is at room temperature, while recovery to baseline was achieved at 100 ˚C. MoS_2 lies on top of carbon nanotubes resulting in a very high value of sensitivity due to their exposed edges. NO_2 was adsorbed from all the directions on exposed edges of MoS_2 along with carbon nanotubes. The device has the detection capability in parts per billion at room temperature. Figure 1.32(b) shows the sensing performance of the heterostructure to 25 ppb NO_2 at room temperature. The gas-sensing performance of the hybrid is significantly improved as compared to pristine MoS_2 and carbon nanotubes.

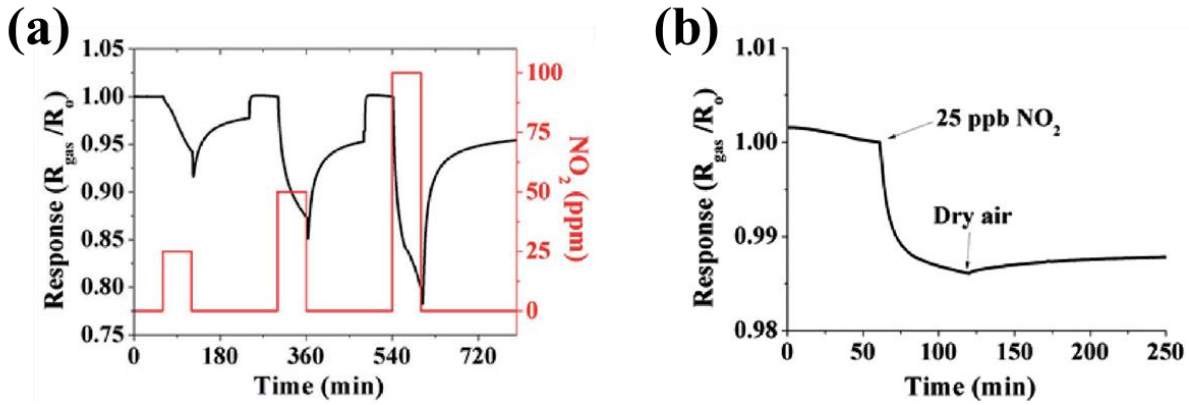

Figure 1.32: Sensing performance of the MoS_2/carbon nanotube hybrid structure against (a) various concentrations of NO_2 gas and (b) 25 ppb concentration of NO_2 gas. (Source: Deokar et al., 2017)

The functionalization of 2D materials through 1D nanostructures is one of the prominent techniques to improve the sensing performance of the device. Ko et al. have exposed the improvement in sensing ability of two-dimensional WS_2 nanosheet through the functionalization of one-dimensional Ag nanowires, as shown in Figure 1.33(a)(Ko et al., 2016). WS_2 was grown using sulfurization of the atomic layer deposited WO_3 film, while Ag nanowire was synthesized by polyol process. Only WS_2 based gas sensors suffer from a poor response and incomplete recovery at room temperature due to strongly adsorbed gas molecules on the WS_2 surface. The presence of Ag nanowires improves the sensing response and makes it completely recoverable even at room temperature. The sensing performance of the device upon NO_2 exposure is shown in Figure 1.33(b). The gas sensing response in Ag nanowire/WS_2 sensor improves by a factor of ~7 than that of pristine WS_2 (Figure 1.33(c)) because Ag enhances the adsorption of NO_2 molecules by creating intermediate states. However, the current level in Ag nanowire/WS_2 device decreases as compared to pristine WS_2 due to the decreasing number of holes through electrons transfer from Ag nanowire to WS_2. In Ag nanowire/WS_2 sensor, NO_2 extracts more electrons ascribed to a higher concentration of electrons in WS_2 resulting from electron transfer from Ag nanowire, as shown in Figure 1.33(d). Therefore, a significant improvement in the sensing ability of a device can be achieved due to the synergetic effect of different dimensional materials.

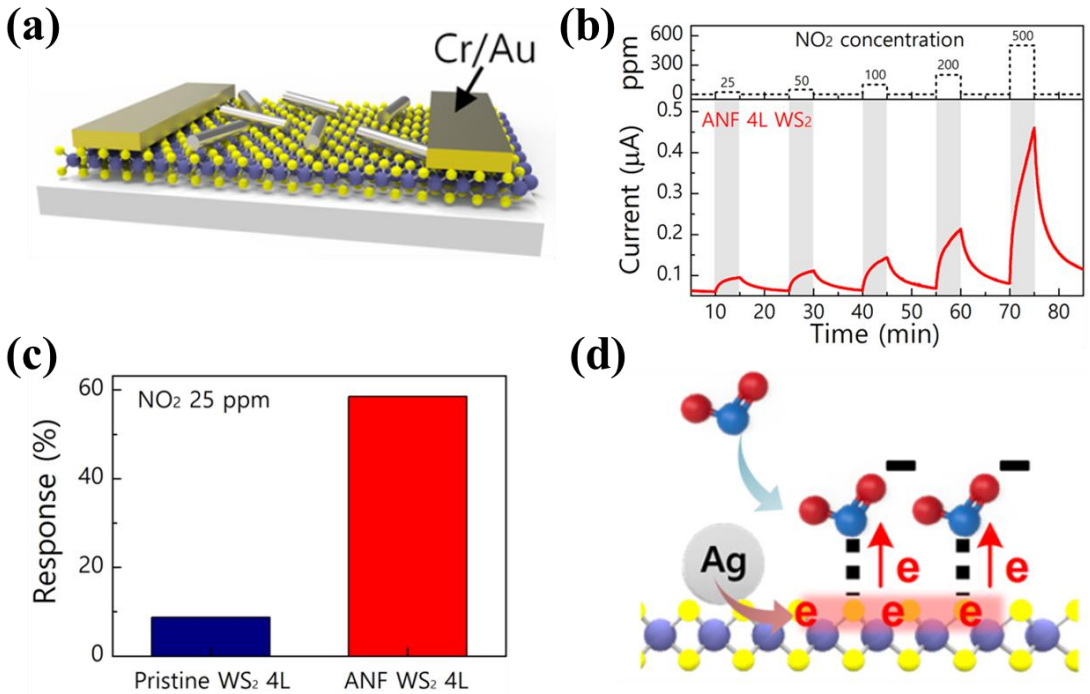

Figure 1.33: (a) Schematic diagram of Ag nanowire/WS_2 sensor. (b) The gas-sensing performance of the device against various concentrations of NO_2 at room temperature. (c) Comparison of sensing response of pristine WS_2 and Ag nanowire/WS_2 based gas sensors. (d) Sensing mechanism occurring at Ag nanowire/WS_2 based sensor. (Source: Ko et al., 2016)

1.6.3 Applications of 2D/2D heterostructures

The 2D/2D heterostructures are synthesized by stacking atomically thin flakes of different 2D materials. The properties of these heterostructures can be engineered even by changing the stacking orientation of the constituent materials. These heterostructures can be formed either by directly growing the two or more materials on top of one another or by growing them on a different substrate and then transferring them at the desired position using various processes. Due to their efficient charge transfer process at the 2D/2D interface, these heterostructures can be used for a large number of electronic and optoelectronic applications.

A large scale 2D/2D heterostructure was demonstrated by forming a MoS_2/graphene based phototransistor as depicted in Figure 1.34(a)(Chen et al., 2016). A centimeter-scale MoS_2 film was synthesized by the low-pressure chemical vapor deposition technique. The MoS_2/graphene heterostructure was formed by two techniques. Firstly, by growing MoS_2 on graphene (G-MoS_2), and secondly by transferring MoS_2 on graphene (T-MoS_2). A comparative analysis of photocurrent on both the device is shown in Figure 1.34(b). The photocurrent is linearly related to the applied drain voltage. The photoresponsivity is one order of magnitude higher in G-MoS_2 based heterostructures is compared to T-MoS_2 based devices. A photoresponsivity of 32 mA/W was observed with excellent stability in G-MoS_2 based phototransistors, as depicted in Figure 1.34(c). The higher value of photoresponsivity is due to the high-quality interface present at G-MoS_2/graphene junction. The high-quality interface facilitates smooth carrier transport across the heterointerface. In G-MoS_2 based devices, the photoinduced electron moves from MoS_2 to graphene efficiently. In contrast, T-MoS_2 based devices hamper the movement of charge carriers due to the presence of wrinkles or surface defects at the interface. The transient response of both devices is shown in Figure 1.34(d). Due to the improved charge transport process, G-MoS_2 based devices exhibit a much faster response. The obtained key feature of the phototransistor can further be improved by improving the quality of the heterointerface.

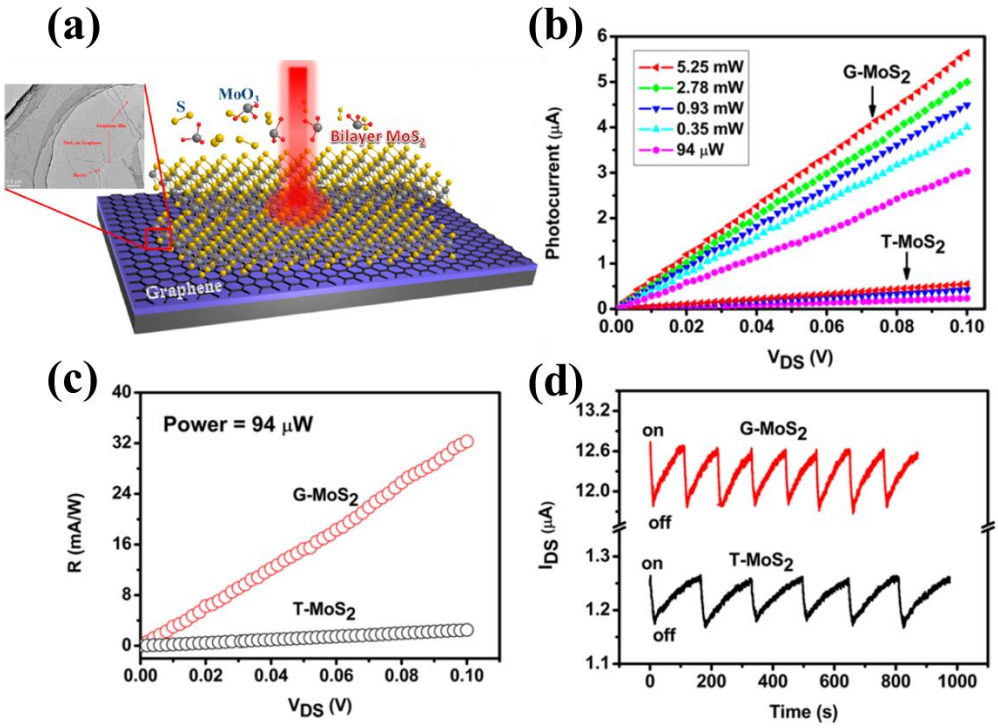

Figure 1.34: Schematic representation of MoS_2/graphene phototransistor. The inset shows the TEM image of the heterostructure. (b) Photocurrent of MoS_2/graphene heterostructure under 650 nm light irradiation at different illumination intensities. (c) Measured photoresponsivity and (d) transient response of the device under 94 μW light illumination. (Source: Chen et al., 2016)

An improvement in MoS_2/graphene heterostructure was obtained using another graphene layer and sandwiching MoS_2 between two graphene layers. A highly efficient graphene/MoS_2/graphene heterostructure based photodetector was demonstrated by Yu et al., as shown in Figure 1.35(Yu et al., 2013). They demonstrated a gate modulated photocurrent across the vertical heterostructure. They controlled the generation of carriers under light irradiation, their separation, and transport mechanism via an applied electric field at a gate terminal. The barrier height at the graphene/MoS_2 heterointerface can be tuned through this gate terminal resulting in controlling of photocurrent generation. Moreover, high photon absorption and efficient charge separation at graphene/MoS_2/graphene heterostructure lead to a higher value of quantum efficiency.

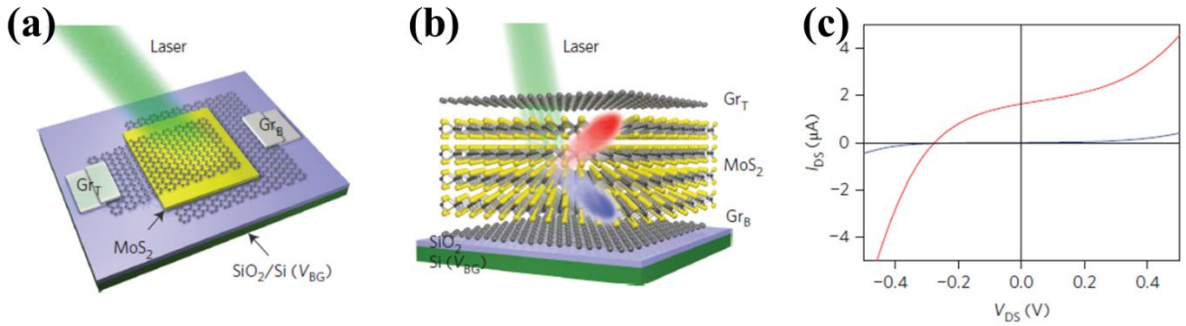

Figure 1.35: Schematic illustration of (a) top view and (b) side view of graphene–MoS_2–graphene heterostructure. (c) Current-voltage characteristic of the device in the dark and under 514 nm light irradiation. (Source: Yu et al., 2013)

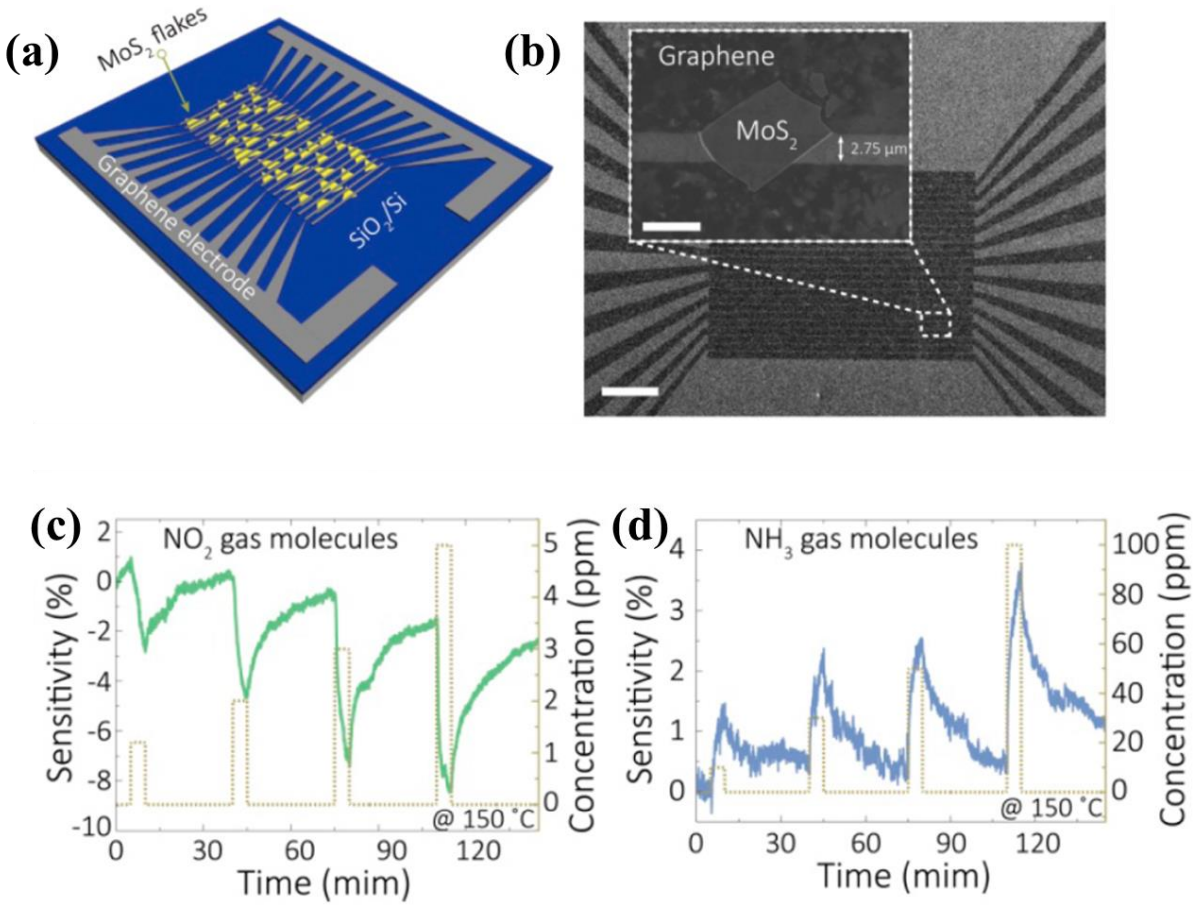

Figure 1.36: (a) Schematic illustration and (b) SEM image of graphene/MoS_2 heterostructure based gas sensor. The sensitivity of the device under the varying concentration of (c) NO_2 and (d) NH_3 gas molecules. (Source: Cho et al., 2015)

The MoS_2/graphene combination is very popular among researchers. Therefore, several dimensional of this combination has been explored in various fields. Cho et al. have explored the gas sensing behavior of graphene/MoS_2 heterostructure devices with excellent gas-sensing stability(Cho et al., 2015). MoS_2 was grown using a mechanical exfoliation technique, while graphene was synthesized by the CVD process. To make MoS_2/graphene heterostructure, the CVD grown graphene was transferred on exfoliated MoS_2 flakes. Figure 1.36(a) and 1.36(b) represent the schematic illustration and SEM image of the sensor depicting graphene electrodes on top of exfoliated MoS_2 flakes. The fabricated device can detect as low as 1.2 ppm concentration of NO_2 with excellent stability. The sensitivity of the device under different concentrations of NO_2 and NH_3 is shown in Figure 1.36(c and d). Due to the higher binding energy of NO_2 molecules, NO_2 could be detected even in very low concentration than that of NH_3.

1.6.4 Applications of 2D/3D heterostructures

The conventional 3D materials are illustrated by schematic diagrams in Figure 1.37(Jariwala et al., 2017). The traditional 3D/3D heterostructures have already shown their enhanced functionalities for modern electronic applications. To explore new functionalities, researchers have replaced one of the 3D components by recently discovered 2D material, forming 2D/3D heterostructures. These newly developed n-n and p-n heterojunctions are widely used for optoelectronic and gas sensing applications. In these kinds of heterostructures, the synergistic effect overcomes the individual limitations of the constituent materials.

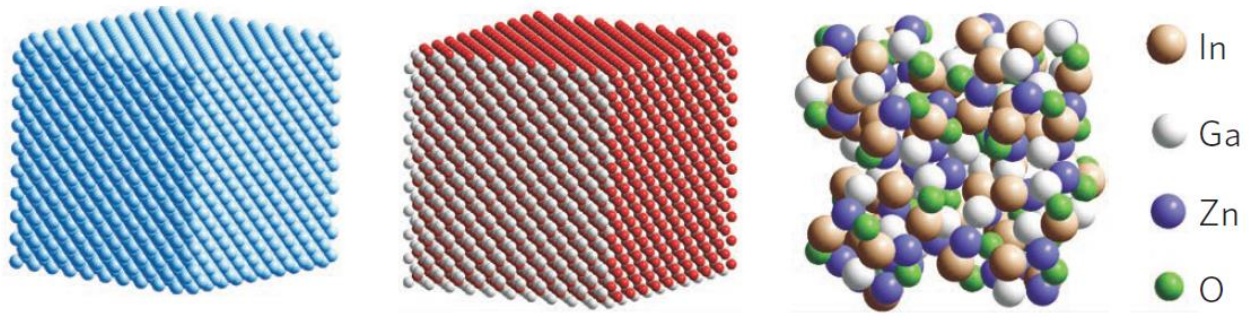

Figure 1.37: Schematic illustration of 3D structures, including Si, GaAs, and amorphous oxides. (Source: Jariwala et al., 2016)

A broadband photodetection from UV to infrared range using germanium-graphene heterostructure based photodetector was demonstrated by Yang et al.(Yang et al., 2017). Germanium, and graphene was grown using CVD technique, and for the synthesis of the heterostructure, graphene was transferred from the copper foil on top of germanium. Photogain and photoresponsivity of several orders higher than that of pure germanium and pure graphene were achieved using the heterostructure. The improvement in photo sensing behavior is due to the efficient generation and separation of photoinduced charge carriers at the heterointerface. The schematic representation of germanium/graphene photodetector is shown in Figure 1.38(a). Graphene does not have a bandgap and forms a Schottky barrier at the germanium/graphene interface, as illustrated by the energy band diagram in Figure 1.38(b). upon light irradiation, photoinduced carriers move from graphene to germanium. The accumulation of electrons through electron transfer from graphene to photoinduced charge carriers in germanium itself leads to a remarkably high value of photocurrent. A maximum responsivity of 66.2 A/W was achieved under 532 nm light irradiation. A comparative analysis of responsivity and photoconductive gain under varying intensities of different wavelengths is

shown in Figure 1.38(c) and 1.38(d). These germaniums based photodetectors are particularly useful for telecommunication applications because of the inherent properties of germanium.

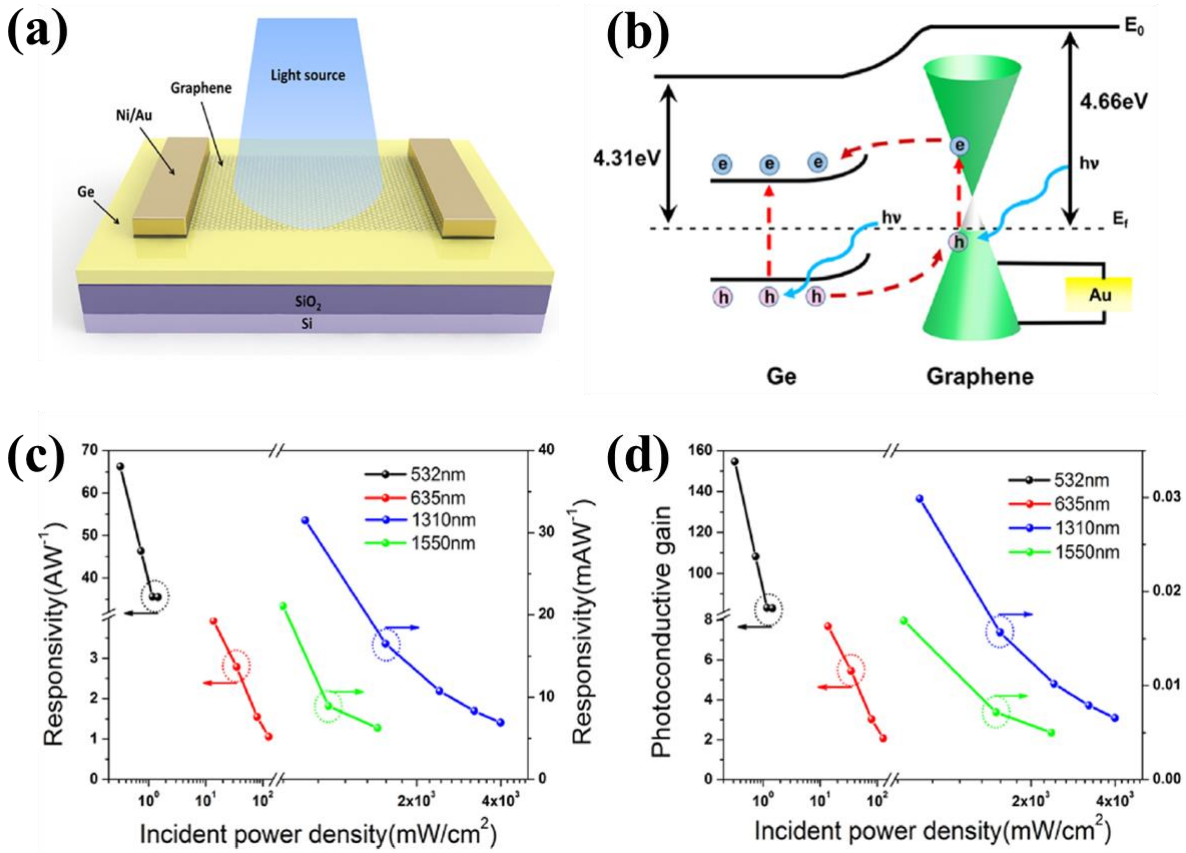

Figure 1.38: (a) Schematic illustration of germanium-graphene heterostructure based photodetector. (b) Band alignment at germanium-graphene heterointerface depicting the movement of photoinduced charge carriers. (c) Photoresponsivity and (d) photoconductive gain of the device at different wavelengths under varying illumination intensities. (Source: Yang et al., 2017)

The photo-sensing performance of 2D/3D heterostructures can further be enhanced by several physical phenomena such as piezophototronic effect. Xue et al. have synthesized a MoS_2/ZnO p-n heterojunction showing a high photoresponse(Xue et al., 2016). A multilayer MoS_2 was grown using mechanical exfoliation, and ZnO was synthesized by a pulsed laser deposition method. To make the MoS_2 p-type, it was doped through the SF_6 plasma treatment technique. The schematic illustration and photoresponse of the device without any gate voltage is shown in Figure 1.39(a). The drain current increases with an increase in the intensity of light irradiation. The photocurrent under 365 nm light irradiation at a different values of drain voltage is shown in Figure 1.39(b). Moreover, piezophototronic effect is used to make the carrier transport more efficient across the heterointerface by lowering the barrier at the MoS_2/ZnO interface. Due to increased pressure, quantum efficiency improves by a factor of four at a pressure of 23 MPa.

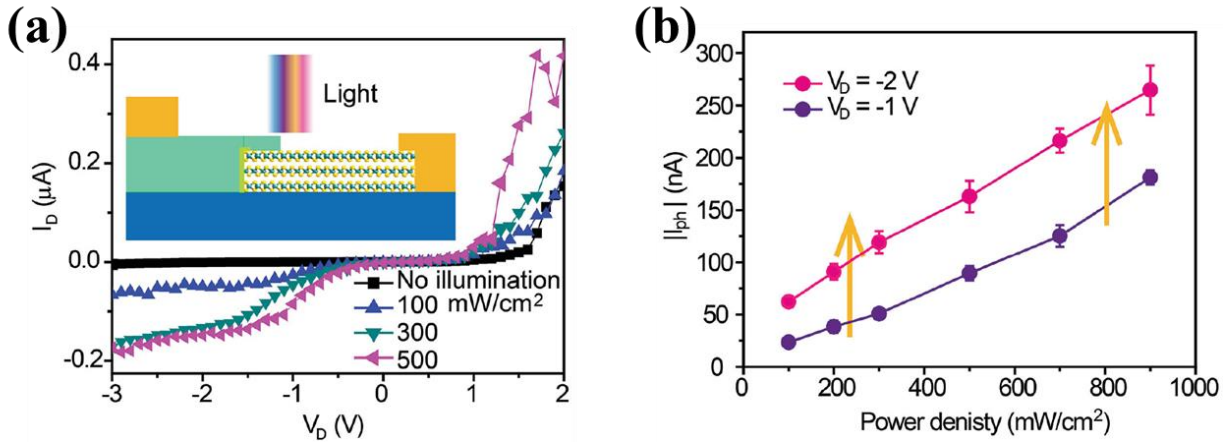

Figure 1.39: (a) Schematic illustration and photoresponse of MoS_2/ZnO heterostructure based photodiode. The I_D-V_D characteristics without illumination and under 365 nm light irradiation with varying light intensities. (b) The photocurrent at a different value of light irradiation intensities at a different value of drain voltage. (Source: Xue et al., 2016)

Not only p-n but n-n type heterostructure are also very popular for photo-sensing applications. A MoS_2/VO_2 n-n heterojunction for its efficient photo-sensing ability was demonstrated by Oliva et al.(Oliva et al., 2017). VO_2 was deposited on SiO2/Si substrate using the magnetron sputtering technique, and multilayer MoS_2 flakes were grown by chemical vapor transport process as displayed in Figure 140(a). The heterostructure depicts a strong rectifying behavior, which eventually turns into Schottky behavior by changing VO_2 from insulating to metallic nature through an external stimulus. A type-II band alignment occurs at MoS_2/VO_2 heterointerface, as shown in Figure 1.40(b). An n-n type heterojunction is formed between MoS_2 and insulating VO_2. Due to their different work functions, electrons start transferring from MoS_2 to VO_2 after forming the contact. VO_2 shows a phase transition from insulating to metallic at 68 ˚C. Once VO_2 turns into a metallic phase, a significant current increases at the heterointerface due to its bandgap collapsing, as shown in the band diagram at MoS_2/VO_2 interface (Figure 1.40(b)). The effect of temperature on photoresponsivity is also studied and shown in Figure 1.40(c). The photoresponsivity increases with an increase in temperature, and it saturates after VO_2 transition from insulating to metallic phase. With the rise in temperature, VO_2 work function increases, which results in a high value of the electric field at the heterointerface assisting in separation of photoinduced charge carriers, and hence high value of photoresponsivity was achieved. Therefore, such kind of phase transition is very useful for the high photovoltaic performance of devices.

These 2D/3D heterostructures have touched every sphere of our daily life, including environmental monitoring. Singh et al. have demonstrated an ultra-sensitive graphene/si heterojunction based gas sensor(Singh et al., 2014). Graphene was grown on Cu foil using conventional CVD technique and then transferred on the substrate, forming graphene/si device, as shown in Figure 1.41(a). In reverse bias conditions, the current depends exponentially on the barrier height at the interface. Therefore, even a small change in barrier height leads to a large variation in current and hence the sensitivity. However, under forward bias conditions, no exponential dependence was observed due to the dominance of the series resistance of the diode. The band alignment at graphene/si heterostructure is shown in Figure 1.41(b). Upon exposure to NO_2 and NH_3 gas molecules, the barrier height at the heterointerface changes resulting in a large change in current. Figure 1.41(c) and 1.41(d) compares the sensing performance of only graphene and graphene/si based gas sensor upon exposure to NO_2 and NH_3 gases. Upon NO_2 exposure, a 13 times improved response was observed in graphene/si heterojunction based devices compared to only graphene-based devices. Due to reverse bias operation, the graphene/si sensor consumes power in μW range compared to conventional gas sensors consuming power in mW range, making it a perfect candidate for low power applications.

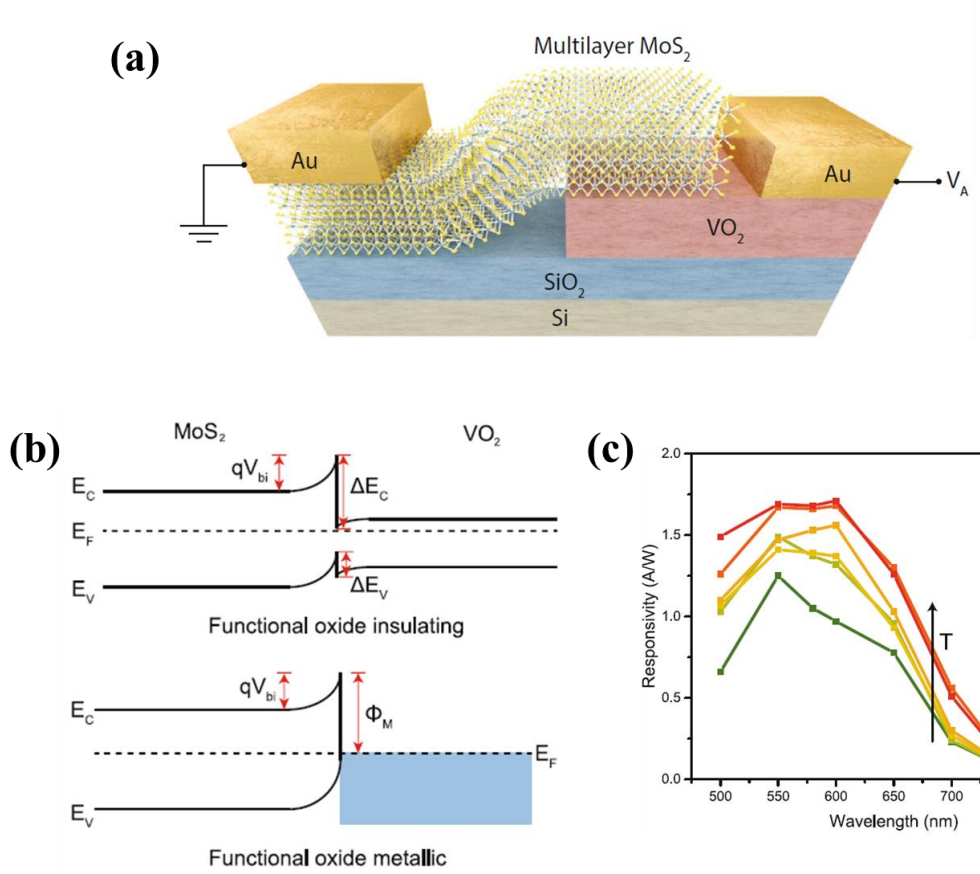

Figure 1.40: (a) 3D schematic representation of MoS_2/VO_2 van der Waals heterostructure. (b) Band alignment at the MoS_2/VO_2 heterointerface when VO_2 is having insulating behavior and after making the transition from insulating to metallic phase. (c) Photoresponsivity as a function of temperature. The photoresponsivity saturates after the phase transition of VO_2 from insulating to metallic. (Source: Oliva et al., 2017)

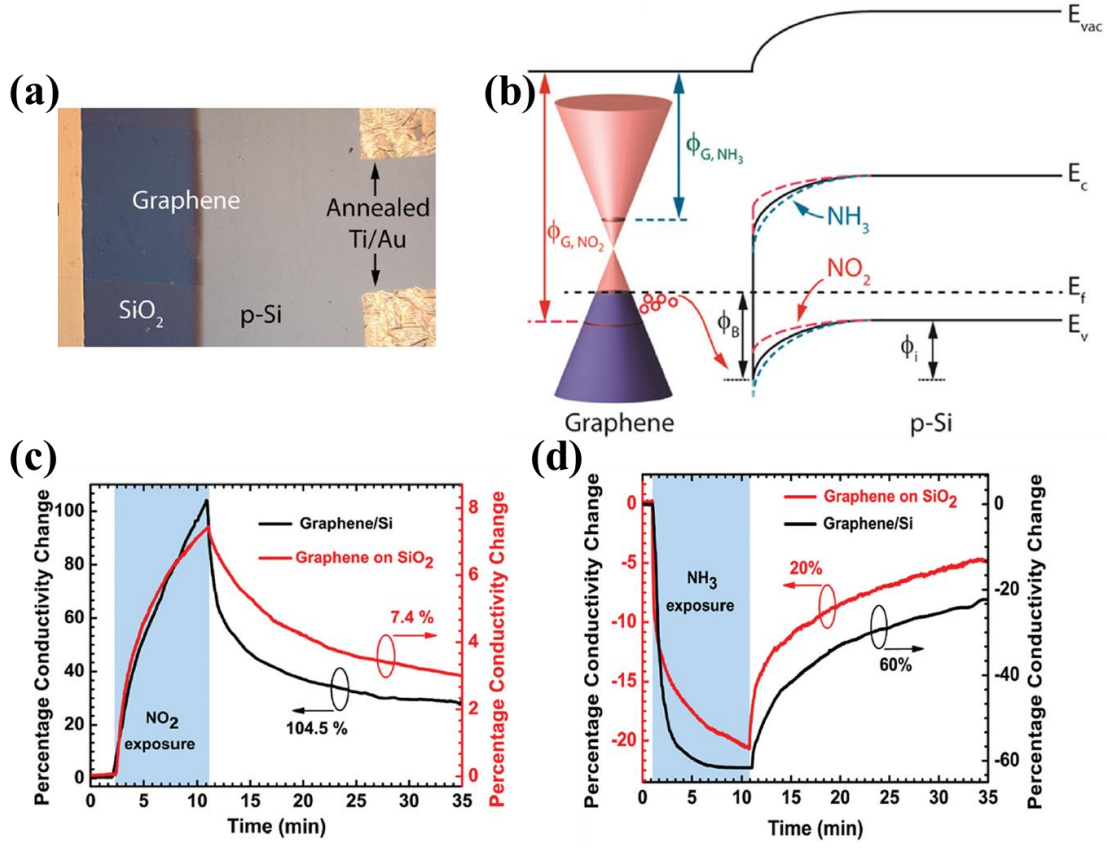

Figure 1.41: (a) Optical image of graphene/si based gas sensor. (b) Band alignment at graphene/si heterointerface. The barrier height at the interface changes upon NO_2 and NH_3 exposure. (c) Comparison of sensing response in the only graphene and graphene/si based gas sensor upon NO_2 exposure. (d) Comparison of sensing response in the only graphene and graphene/si based gas sensor upon NH_3 exposure. (Source: Singh et al., 2014)

1.7 MOTIVATION

In 1965, Gordon Moore stated that the number of transistors on a chip doubles every two years. Over the last five decades, Moore's law works reasonably well, driving the significant improvement in performance and a sharp decrease in prices of electronic circuits. Miniaturization has led to a tremendous increase in device functionality per unit area. But now Moore's law starts saturating mainly due to excessive heat generated within the chip(Mack, 2011). The occurrence of substantial leakage or off current in the devices severely deteriorated their functionalities. Decreasing the dimensions of the device has further aggravated the problem. Although several efforts have already been put in place for improving the device performances, for instance, uses of high-k dielectric and bi- and tri-gate transistors. However, these advancements have their own limitations(Lee et al., 1999; Lu et al., 2012).

To revive Moore's law, the scientific community has to look beyond the conventional semiconductors below the 10-nm node for making high performance and low dimension electronic devices. The atomically thinned layered materials popularly known as two dimensional (2D) materials showed a high probability of bringing back Moore's law to life. By the discovery of graphene in 2004 by Professor Andre Geim and his Ph.D. student Kostya Novoselov at the University of Manchester led to the birth of a new class of material called 2D materials. They isolated graphene from the graphite crystal by using micromechanical exfoliation technique(Geim and Novoselov, 2010; Novoselov et al., 2004). The new class of materials where the thickness is negligibly small or the third dimension is absent is known as 2D materials. Since the isolation of graphene (the mother of all 2D material), numerous other 2D materials have been explored for their wide range of applications in nano-electronic and photonic devices(Gupta et al., 2015; Zhang et al., 2016).

Nonetheless, the absence of bandgap in graphene poses some restrictions on the uses of graphene(Echtermeyer et al., 2008). Therefore, several other materials have been discovered to address the challenges faced by graphene. The properties of these 2D materials are utterly distinct from their bulk counterpart. The bandgap, electron mobility, and contact resistance change very rapidly as the bulk semiconductors thinned down to a few-layer or monolayer thickness. Similar to graphene, MoS_2, one of the most extensively studied 2D semiconductors, also grabbed huge attention due to its unique electronic, optical, mechanical, and chemical properties(Li et al., 2017; Son et al., 2015; Yim et al., 2014). Even in some of the specific applications, MoS_2 outperforms graphene primarily due to the availability of bandgap in the former, which is an essential ingredient for digital electronics applications. MoS_2 is having an indirect bandgap of ~ 1.2 eV in its bulk form, which makes a sharp transition to a direct bandgap of ~ 1.8 eV in its single-layer form(Mak et al., 2010). In addition to the change in the bandgap, MoS_2 possesses several exciting layer-dependent attributes, which makes it a suitable candidate for novel electronic devices. In recent years, MoS_2 establishes itself as the promising gas-sensing material due to its large surface-to-volume ratio and very simple sensing mechanism based on a change in resistance of the material(Donarelli et al., 2015; Kumar et al., 2017).

In recent years, the limited applications of isolated 2D materials have inspired the researchers to explore van der Waals (vdW) heterojunctions of these 2D layered materials with other materials(Jariwala et al., 2016; Schulman et al., 2017; Srisonphan, 2016). These vdW heterojunctions become very popular within a short span of time because of their dangling-bond-free surface, tunable properties, and cutting-edge over the conventional semiconductor devices. These heterojunctions also relax the constraints of lattice matching, thus increasing

their versatility for various potential applications(Jariwala et al., 2016). Nowadays, MoS_2, being one of the most intensively researched 2D materials, received remarkable consideration for its mixed dimensional heterojunction based applications because of its unique inherited merits, including its unconventional mechanical, physical and structural properties(Lembke et al., 2015; Yoon et al., 2011). A significant effort has been devoted to integrating MoS_2 with other materials to tune the properties of interface for desired applications, for instance, light-harvesting and light-emitting devices(Li et al., 2017), high-performance sensors(Kumar et al., 2017), solar cells(Tsai et al., 2014), and novel diodes(Schulman et al., 2017). Gong et al.(Gong et al., 2014) demonstrated a single-step growth strategy for fabrication of seamless and atomically sharp in-plane heterostructure of MoS_2 and WS_2 under different growth temperatures to explore new possibilities of 2D materials. A 2D/3D heterojunction based on the growth of MoS_2 on GaN was reported by Ruzmetov et al.(Ruzmetov et al., 2016) to create complex structures for the implementation of high-performance electronic devices. The integration of these 2D layered materials with other materials extensively addresses the challenges faced by a new generation of optoelectronic and photovoltaic devices. Some of the key applications of these heterostructures are shown in Figure 1.42. Therefore, in this thesis work we have investigated the suitability of 2D/3D heterojunctions for photo and gas sensing applications.

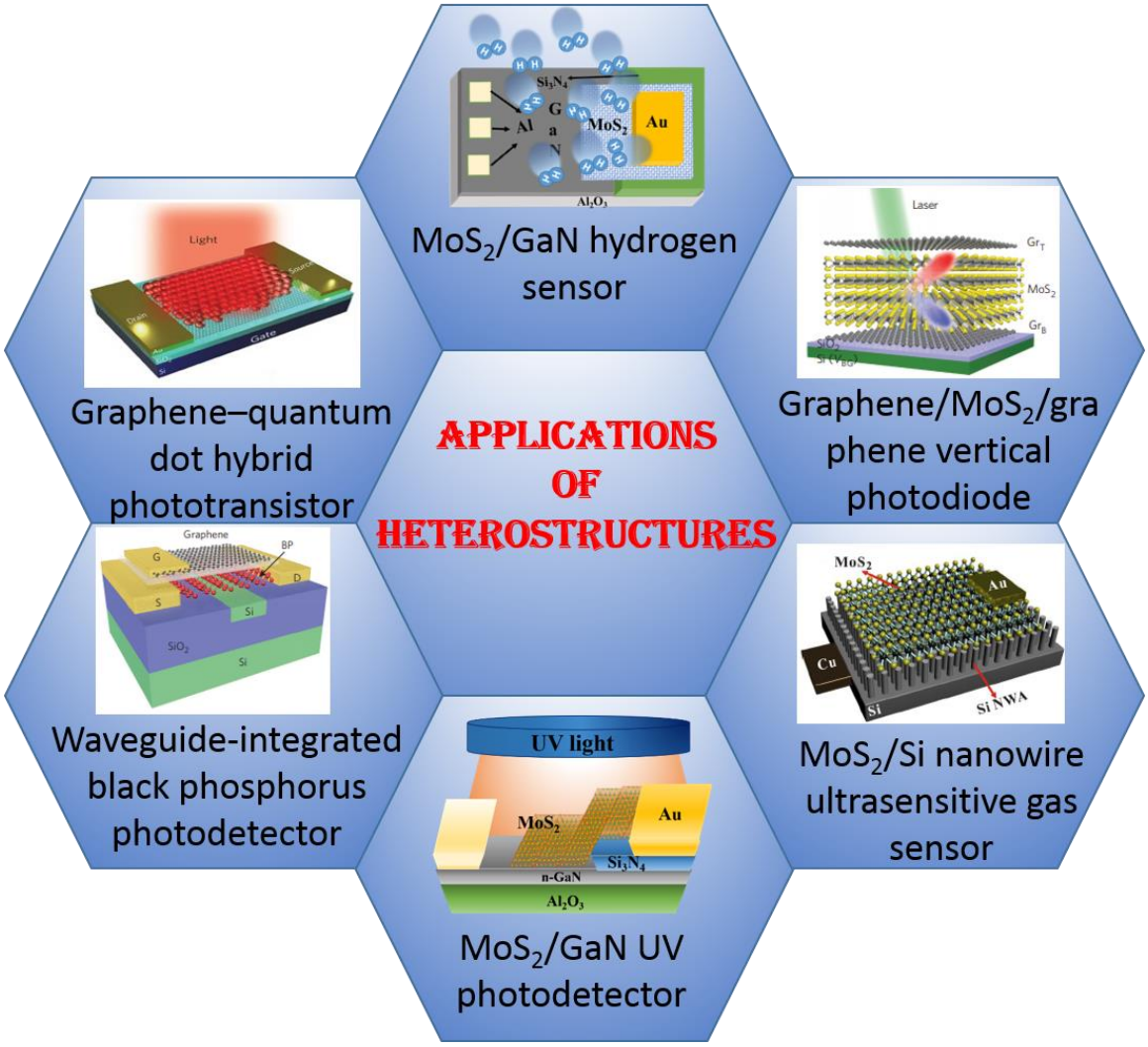

Figure 1.42: Some of the key application of Heterostructures heaving atleast on 2D component.

1.8 OBJECTIVES OF THIS WORK

The very visionary American physicist Richard Feynman in his very famous talk "There's plenty of room at the bottom" in 1959 asked, "what could we do with layered

structures with just the right layers?" After the relentless efforts over several decades, we are able to answer that question(Ajayan et al., 2016). Nowadays, we are experiencing Feynman's vision by creating heterostructures using atomically thin layers of various materials. These heterostructures can easily be created and manipulated according to a specific application. In these heterojunctions, the conventional constraint of crystal lattice matching is relaxed. The relaxation in lattice matching allows integration of any 2D layered materials and realizing those applications which were previously not possible with conventional semiconductors.

The main goal of this thesis is to use MoS_2 based heterojunctions specifically for optical and gas sensing applications. The objectives to accomplish this goal have been identified as:

- To grow high-quality few-layer MoS_2 film over various substrates through different techniques
- To optimize the growth parameters for achieving high-quality MoS_2 film
- To characterize the fabricated MoS_2 film through various microscopic and spectroscopic measurements
- To study the band alignments at MoS_2/Si and MoS_2/GaN heterojunctions
- To analyze the charge transport and carrier dynamics at the heterojunctions
- To study the optical performances of the heterojunctions
- To evaluate the gas sensing performance of MoS2/GaN heterojunction

1.9 ORGANIZATION OF THIS THESIS

This thesis work includes various 2D/3D heterojunctions primarily focusing on MoS_2 as a 2D material. We demonstrate the uses of these heterojunctions particularly in the field of optical and gas sensing applications. This thesis is organized in 8 chapters, the outline of this thesis is described below:

Chapter 1: This chapter summarizes the literature review, which forms the foundation of the work done in this thesis. It explains the recent advances in the field of 2D materials. Here, we have also mentioned some of the major milestones achieved in the area of 2D materials. The different properties of 2D materials, making them suitable for a particular application have also been discussed in this chapter. In this chapter, we explained the heterostructures formed by combining different dimensional materials and their unique advantages to address the formidable challenges faced by the electronic industry. Lastly, we describe the motivation and specific objectives of this thesis work.

Chapter 2: This chapter involved various synthesis and characterization techniques used in this thesis work. Mechanical exfoliation and sputtering coupled with sulfurization are the main techniques used for the growth of 2D material during device fabrication in this thesis work. While the characterization involves mainly field emission scanning electron microscopy (FE-SEM), atomic force microscopy (AFM), optical microscopy, X-ray photoelectron spectroscopy (XPS), Ultraviolet Photoelectron Spectroscopy (UPS), and Raman characterization techniques.

Chapter 3: In this chapter, we visualized the band alignments across the MoS_2/Si and MoS_2/GaN heterojunctions for determining the type of heterojunction at the interfaces. The valence and conduction band offsets have been calculated using X-ray and Ultraviolet photoelectron spectroscopy techniques.

Chapter 4: In this chapter, we have studied various scattering mechanisms to understand the contribution of different carrier interactions in the conduction process. The modulation of barrier height at the heterointerface due to light irradiation has also been explained in this chapter.

Chapter 5: This chapter explains a 2D/3D heterojunction type photodetector by depositing MoS_2 on a GaN substrate. A high value of external spectral responsivity and detectivity unveils a new perspective in MoS_2/GaN heterojunctions for high-performance optoelectronic applications.

Chapter 6: In this chapter, we report a MoS_2/GaN heterojunction based hydrogen gas sensor. A very high value of sensitivity due to the tuning of barrier height at the heterointerface upon hydrogen exposure is also explained in this chapter. The proposed methodology can readily be applied to other combinations of heterostructures for sensing different gas analytes.

Chapter 7: In this chapter, we have studied charge transport mechanism and the device physics under thermal excitation.

Chapter 8: This chapter summarized this thesis work and gave the future perspective of low dimensional materials, particularly in the field of optical and gas sensors.

…